SCHOOL OF EARTH SCIENCES

GEOLOGY AND STABILITY OF OPAL FROM WEGEL TENA AREA, ETHIOPIA.

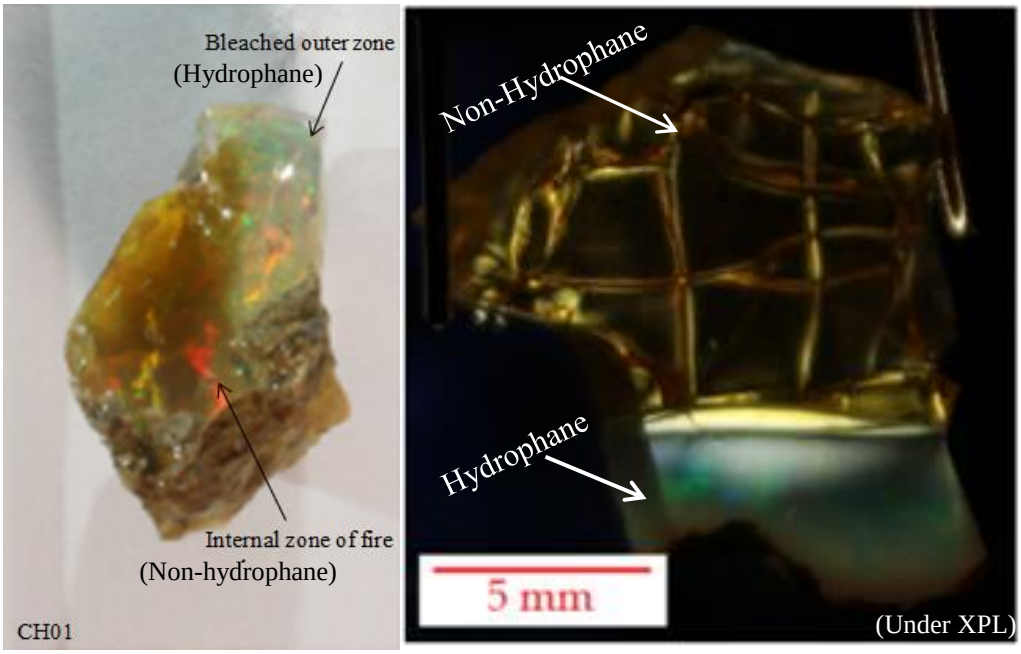

A THESIS SUBMITTED TO THE SCHOOL OF EARTH SCIENCES ADDIS ABABA UNIVERSITY IN PARTIAL FULFILMENT OF THE REQUIREMENTS FOR THE DEGREE OF MASTERS OF SCIENCE IN MINING GEOLOGY

SELAMAWIT DAGNACHEW

ADVISORS: - PROFESSOR DEREJE AYALEW

Dr. WORASH GETANEH

PROFESSOR BENJAMIN RONDEAU

NOVEMBER ,2017

ABBIS ABABA

GEOLOGY AND STABILITY OF OPAL FROM WEGEL TENA AREA, ETHIOPIA.

A THESIS SUBMITTED TO THE SCHOOL OF EARTH SCIENCES ADDIS ABABA UNIVERSITY IN PARTIAL FULFILMENT OF THE REQUIREMENTS FOR THE DEGREE OF MASTERS OF SCIENCE IN MINING GEOLOGY

BY SELAMAWIT DAGNACHEW

ADVISORS: - PROFESSOR DEREJE AYALEW

Dr. WORASH GETANEH

PROFESSOR BENJAMIN RONDEAU

NOVEMBER, 2017

ADDIS ABABA UNIVERSITY

SCHOOL OF EARTH SCIENCES

GEOLOGY AND STABILITY OF OPAL FROM WEGEL TENA AREA, ETHIOPIA.

BY SELAMAWIT DAGNACHEW

DEPARTMENT OF EARTH SCIENCES

APPROVED BY THE EXAMINING BOARD

_____ ----------

Chairman, Department

Graduate committee

PROFESSOR DEREJE AYALEW ----------

Advisor

Dr. WORASH GETANEH ----------

Advisor

_____ ----------

Examiner

_____ ----------

Examiner

Acknowledgement

I have no words to express my deepest gratitude to my advisor Professor Dereje Ayalew for his decisive guidance throughout this thesis work and for arranging to conduct the laboratory analysis in Nantes University, France. My deepest gratitude continues for my advisor Dr. Worash Getaneh for his great constructive suggestions and comment to accomplish this work successfully. Moreover, I am highly indebted to Professor Benjamin Roneadu for his support to analyze all laboratory works by himself in University of Nantes, France (Laboratoire de Planétologie et Géodynamique) and providing valuable reference materials and comment over the whole work. Thank you and may God bless you all.

My great full thanks continue to Addis Ababa University, School of Earth Science for providing the fund for the entire work.

My final gratitude goes to Dilla University for sponsoring and giving me this golden opportunity.

CONTENTS

LIST OF FIGURES

LIST OF TABLES

Abstract

Crazing (cracking) is a common opal destabilization which has not been studied in detail prior to this work. It is a major economic issue for the opal gemologic market and the industrial synthesis. The aim of this research is to understand cracking (crazing) phenomena of opals from Wegel Tena locality. To achieve this, opal samples are directly extracted from three different local mining sites of Wegel Tena opal deposit (Koke Wuha to the northeast of Wegel Tena town, Anset to west of Wegel Tena town and Chegen to the north of Wegel Tena town) from the host rocks of rhyolitic ignimbrites. The opal samples have been characterized under natural light, crossed polarizers and Raman spectra data. The opal samples were heated in order to accelerate the evacuation of the water. Hydrophanes opals (KOK01, CH01 bleach zone and AN02) have shown no development of cracks after heating. While non-hydrophanes opals (KOK04, KOK05, internal zone of CH01) develop crack pattern after heating regardless their transparency. All non-hydrophane samples at low Raman spectral resolution ($3cm^{-1}$) showed significant variation at $780cm^{-1}$ peak (up to $13cm^{-1}$), which is an indicator for strong strain into the Si-O-Si bond. The average value for this shift is about $3.3cm^{-1}$ down after crazing (cracking) reflecting extensive stresses impact for crack development. Birefringence patterns (produce extensive local constraint) observed around the cracks between crossed polarizers. Abnormal birefringence figures appear with crazing: anisotropy is created around breaks. Opal stress distribution is dependent to opal surface irregularities and breaks distribution. Water loss triggers crazing into non-hydrophane opals. Crazing reorganizes stress distribution according to the new surface distributions. Generally hydrophanes opals (KOK01, CH01 bleach and AN02) have better resistance to cracking than non-hydrophanes opal (KOK04, KOK05, internal zone of CH01) even at high temperature. In Hydrophane opals water exist in molecular form.

CHAPTE ONE INTRODUCTION

1.1. BACKGROUND OF THE STUDY

Opal is an amorphous (opal-A) or poorly crystalline (opal-CT) variety of hydrous silica, $SiO_2.nH_2O$. The "n" indicates that it contains an indefinite amount of water (Aguilar-Reyes, 2004; Paris et al., 2006). The water content ranges commonly from 6% to 13% weight. Opal measures 5.5 to 6.5 on Moh's hardness scale with pearls 4 to 5 and diamonds measuring 10 (Paris et al., 2006).

The presence of opal in the earth crust can be found in numerous places; however some occurrences are inaccessible others are still likely to be discovered (Rondeau et al., 2011b). The noble opals are the opals most appreciated for their quality gem and their colors of iridescence. Gem-quality opals for the most part come from two types of deposits: volcanic and sedimentary (Frondel, 1962).

The discovery of Ethiopian opal appeared on the market in the mid-1990s. Specimens from Mezezo in the historical Shewa province consist of nodules of a reddish brown volcanic rock with orange, reddish brown, or chocolate brown precious opal inside (Mary et al., 1996). The next major discovery occurred in 2008, when white precious opal was found in the province of Wollo near Wegel Tena. Unlike previous Ethiopian opals, the new material is mostly white, with some brown opal, fire opal, and colorless "crystal" opal (Mazzero et al., 2009). The percentage of gem quality material is surprisingly high in this deposit. Many samples are of outstanding beauty and value unlike most opals in the market today (Rondeau et al., 2012).

Basically the best qualified deposit compared to the international standard is found at the Shewa province around Mezezo area and in the Amhara region of Wollo Wegel Tena provenance (Mary et al., 1996). The geologic conditions under which opals formed at these areas share common characteristics. However, the disposition of opal in its host rock differs between the two localities. At Wegel Tena opal most often cements volcanic grains, while at Mezezo it usually forms nodules filling the cavities in volcanic rock. The Wegel Tena is a source of significant quantities of high-quality play-of-color opal, with a mostly white body color that is more market-friendly than the mostly brown material from Mezezo ~200 km to

the South. Gem opals from Wegel Tena, Wollo Province, Ethiopia, occur in Oligocene rhyolitic ignimbrites (Rondeau et al., 2012).

Gem-quality opal with satisfactory structural stability, durability, play of color, color saturation and color patterns make people aspiration higher to use it as jewelers, personal adornment. Due to these demands, precious opal has become an important mineral commodity (Seid, 2006). Any mineral or gem material is considered unstable if some of its physical properties change with time. Color, transparency, and cohesion are the main properties that are susceptible to change. Opal is a mineral that can be stable: some archaeological specimens remain stable several thousand years after their extraction. However, in some cases, opal is unstable for two distinct reasons: some cracks can appear (sometimes even leading to breakage) or an opaque white egg can develop inside a transparent gem. The two phenomena of destabilization are here after called "cracking" and “whitening” respectively (Rondeau et al., 2011a). This phenomenon appears over the time (days, months or years) as related to the extraction date from the mines and in seen with or without unexpected variations of pressure, temperature and occasionally as a consequence of mechanical influence due to polishing. From a mineralogical and genetic standpoint destabilization phenomenon is important because it was likely appeared in solid state after primary formation of the opal deposits. Although the origin of silica modifications in volcanic opals was interpreted to have formed from hydrous silica gel, there are believed to be different transformations in the solid state at low and room temperatures (Ostrooumov, 2007).

Despite the considerable experience of opal miners and dealers, the situation described by Pearson (1985) there seems to have been no objective criterion by which the stability of a particular sample of opal could be predicted, although experienced dealers and cutters frequently have subjective and often unexplainable techniques for assessing stability.

1.2. DESCRIPTION OF THE STUDY AREA

1.2.1. Location and accessibility

The study area is located in Wegel Tena area, which is about a total of 550 km north of Addis Ababa. The locality has also been referred to as “Delanta,” which corresponds to a former

subdivision (or "awraja") of Wollo Province. The area is accessed through Addis Ababa – Desse town main asphalt road, which has a total length of 406km from Addis Ababa, and also additional 150 km gravel road that connects Desse with Wegel Tena town is used to access parts of the study area. Other small towns in the area are connected to each other with networks of dry weathered roads and these roads are used to access different parts of the study areas.

The region containing opal deposit within the area is not restricted in specific locality. In a wide range of area a lot of recently discovered traditional mining sites are distributed in all direction of Wegel Tena town (Chegen area northwest of Wegel Tena, Koke Wuha East of Wegel Tena, Anset North of Wegel Tena). All of the localities cover a large area that encompasses scattered farms and a small locality with less than 17 km of Wegel Tena town. The area is situated on a plateau at an altitude of about 3,200 m. The opal occurs in a horizontal layer that is exposed on a cliff. All the areas are accessible with various transportation systems, and the various mine workings are reached by walking down the steep canyon for 30 minutes to more than one hour. The study area is bounded 11°22'0'' to 11°46'00''N latitude and 39°0'00''E to 36°30'0''E longitude and falls in the Ethiopian Mapping Agency topographic map of GISHEN sheet (1139A4, Edition 1 EMA 1996) and WEGELTENA sheet (1139A3, Edition 1 EMA 1996) 1:50,000 scale.

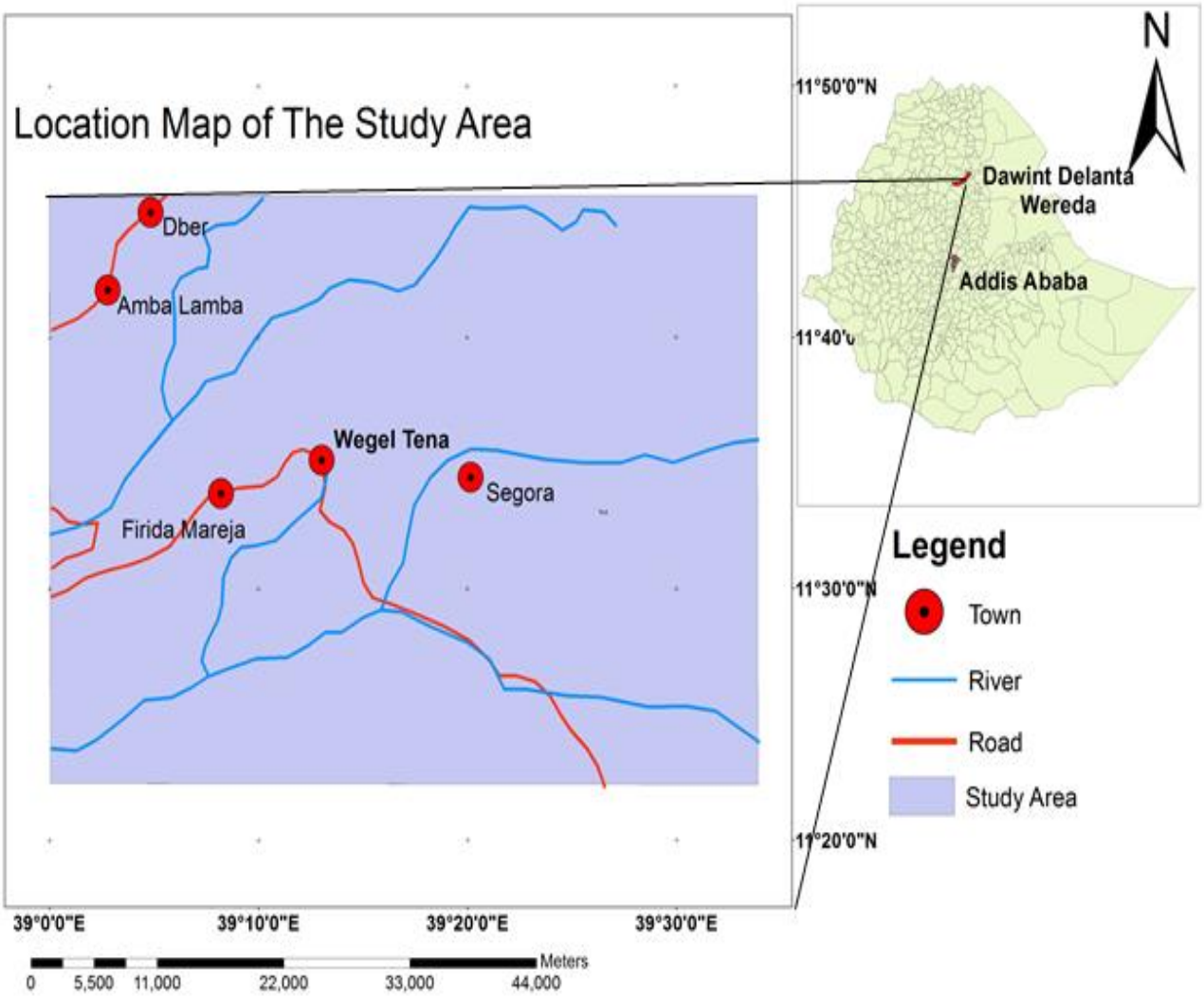

Figure 1.1: Location map of Wegel Tena Wollo provenance, Ethiopia.

1.2.2. Climate

There is no nearby metrological station in the study area therefore the data is taken from the nearby Kombolcha metrological station. According to a rainfall data from Kombolcha metrological station the mean annual rainfall ranges between 614.80mm-968.7 mm. The mean annual temperature is 5.9 – 19.11 ^{0}C with the minimum average ranging from 1.6^{o}C during October to 7.1^{o}C during December and maximum temperature varying from 21.2^{o}C during January to 28.0^{o}c during June. (Source: Delanta Woreda information bureau)

1.2.3. Physiography and Drainage

The study area is characterized by undulating topography with cliff, valleys and gorges. The altitude ranges from 2320m - 3300m a.s.l. Relatively, Northern and Western part of the study area exhibit less difference in elevation that ranges between 2949m-3020m around Tsehay Mewcha locality, but the Southern and Eastern part of the project area shows wide range of elevation difference with average of 2320m at the bottom and in the ridges the elevation becomes high with maximum elevation of 3300m.

The project area has one major perennial river, with its main tributaries and other small tributaries. They form deep gorges which gradually widen into valleys and dendritic to sub – parallel drainage patterns.

1.2.4. Land Use and Land Cover

The Land surface of the study area is covered by different features like; forest, agriculture, bush land, bare land and settlements. Hamusite are covered by shrubs, bushes, small trees and bare lands with exposed rock units except following the rivers banks which is used for agriculture where people grows different vegetation; among them barley and Teff are common ones. In addition small settlement villages were built associated with the cultivated fields. Along the road which connects Wegel Tena, different small towns are built but the rest of the area is covered by forest.

1.3. STATEMENT OF THE PROBLEM

The quality gemstone with satisfactory structural stability, durability, play of color, color saturation and color patterns make people aspiration higher to use it as jewelry, if precious gem stable ,it remain stable for several thousand years after their extraction. However any mineral or gem material is considered unstable if some of its physical properties change with time. Stable Color, transparency, and cohesion are the main properties that are susceptible to change.

According to (Rondeau et al., 2011a) when opal is mined, the samples often appear as nice pieces that seem to promise beautiful cut samples. After a while the samples destabilize, either by cracking or whitening. A phenomenon often referred to as “crazing”. It can occur within a

few hours after mining, or even sometimes after several months. These two phenomena of destabilization of opals are poorly understood because they are little studied, although they affect the whole market of gem opals. Aguilar-Reyes (2004); Aguilar-Reyes et al.(2005) mentioned the following basic reasons for the difficulty of studying opal stability. 1) It is quite difficult to get samples from a very precise provenance and it is also difficult to be certain that, the observed features are due to destabilization. Understanding the exact place where each specimen was brought is very important to characterize the influence of geological formation on destabilization of the opals. Secondly and most importantly the samples must be large enough to perform some destructive tests and such research project requires many analytical methods and procedures. Due to the above mentioned reasons no one is interested performing detail research project work on opal destabilization. So far only a few research works have been conducted around the world concerning destabilization of opal.

Stability of opal is a serious issue for Ethiopian opals. However, the opal tends to destabilize outside of its natural genesis. Once explored during cutting and polishing or even well after its sale on the market, an opal can present two types of loss of gem quality: either by bleaching, or by the appearance of a network of cracks (Rondeau et al., 2011a). This is a major economic problem in the gemological market which cannot guarantee the stability of the parts in the long term.

The study left a huge gap on the stability of opal such as understanding the phenomenon of Wegel Tena opal crazing (cracking). Therefore this research intends to come up with the possible cause of Wegel Tena opal (crazing) cracking phenomena. Besides this, studying opal destabilization in this particular place helps us to put scientific evidence for how time and temperature variation affect stability of opal.

1.4. OBJECTIVE OF THE STUDY

1.4.1. General objective

The basic objective of the research is to understand the cause of crazing (cracking) of opal from Wegel Tena area, Ethiopia.

1.4.2. Specific objective

The specific objectives of the study are:

- To identify factors leading to crazing (cracking) of opal
- To understand the effect of time since extraction on the stability of opal
- To Study the effect of heat on the stability of opal
- To construct the geological map of the area

1.5. METHODOLOGY

In order to achieve the general and specific objectives of this research the following methodology were followed.

1.5.1. Secondary data collection and review of previous relevant works

Before the field work have been conducted the following activity were done.

- Different previous relevant works on Geology, Gemology, petrology and Geochemistry that conducted around the study area reviewed from published or unpublished reports, maps, journals, scientific publications, web sites, etc. And also Books, journals, scientific publications and web sites that conducted in different part of the world specifically that important for this study were reviewed.
- Before the field works were conducted the study area is delineated using Arc GIS software from topographic map of GISHEN sheet (1139A4, Edition 1 EMA 1996) 1:50,000 scale and WEGELTENA sheet (1139A3, Edition 1 EMA 1996) 1:50,000 scale.
- Available information's like temperature, rain fall data, forest coverage and soil coverage, accessibility of the area, topographic set up, and lithological set up of the study area were collected from topographic map, Google Earth, Aerial photo and from different existing data.

1.5.2. Primary Data collection

The field work was conducted from January 8/2017 to January 24/2017 for a total of 16 Days. At the time of field work the traverse sections were selected systematically in order to

encounter different lithological units that believed to be appropriate for rock sampling of the opal host rock and to get many local opal mining sites. Before the actual representative opal sample collections were conducted, a total of two days were spent to gather information about the area and opal mining activity from the local peoples and Wereda level administrative bodies.

During field investigation an attempt was made to describe the geology of the area and representative opal samples in detail at hand specimen scale. A total of 30 opal samples from three different artisanal mining sites were collected (Chegen locality to the north of Wegel Tena town, Koke Wuha northeast of Wegel Tena and Anset to the west of Wegel Tena town). Sampling includes both gem quality and common opals from volcanic deposits of rhyolitic ignimbrite with or without play-of-color. Opal sample collection is mostly focused on very transparent one. All samples are nodules of opal sampled directly on the mining sites, then immediately stored in a closed plastic bottle with water and kept out of direct sunlight or intense light to prevent their possible drying hopefully temporary cracking and whitening.

All of the samples are collected from 100m to 300m long local mining tunnel to avoid any possible previous interaction of samples with the atmosphere. At the time of sampling each samples property (color, crack pattern and optical properties) and stability of gem opal in the opinion of local Miners were recorded. Each sampling stations and lithological contacts GPS readings were recorded and photos of different lithological unites were taken.
Attempts were made to construct detail lithological unit logging during the field work and the closest thickness of each layers were estimated. The sample codes have a prefix, starting with the locality name where the samples are collected from. For example; a sample with prefix "CH" means samples which collected from Chegen locality.

1.5.3. Laboratory analysis

To understand the petrographic property and to see petrographic variations of the opal host rock, six rhyolitic ignimbrite rock samples were sent to central laboratory of Ethiopian geological survey for thin-section analysis.

After the opal samples were collected and stored in a plastic bottle successfully, a total of 30 samples sent to France, University of Nantes Planetology and Geodynamic Laboratory for gemological analysis. From among the 30 collected samples five representative samples were selected on the basis of transparency, homogeneity and variation of mining sites. Firstly the samples physical and optical property and their sense of destabilization have been investigated in room temperature. Then, the selected samples were cut into 2 mm thick slides except KOK04, which is cut to 1 mm thickness. They were polished on one side with diamond 6μm. The cutting, parallelization and polishing of the faces were carried out in the presence of water and by hand to Preventing destabilization.

Photographs have been taken after the samples heated at 150^0c for KOK01, KOK04, KOK05, CH01 and 500^0c temperature for AN02 (maximum temperature at which the highest crack patterns observed in each samples) in order to understand the evolution of their macroscopic aspect. The purpose of heating the sample is to accelerate the evacuation of the water and to observe the spectral variations associated with it. 5 mm wide shards have been made on the thick slats, for a passage in a high temperature cell. The slice samples photographs have been taken under a binocular Leica microscope in transmitted light between crossed polarizers in order to reveal interferences figures indicative of internal stress in opal which later used to interpret crack development.

The Raman properties were measured on a LabRam HR Evolution spectroscope of Horiba Scientific, with a laser at 532nm of 100mW of power (except for KOK05: 50mW). The network used for the acquisition was 300lines/mm ($3cm^{-1}$ spectral resolution). The analyzed spectral windows ranged from 200 to $2000cm^{-1}$ (area of the silica) and 2500 to $4000cm^{-1}$ (water zone). The LabSpec 6 software enabled the automatic acquisition of spectral data in order to measure the spatial variations of the position of the Raman peaks. They were acquired at high temperature via a Linkam cell, at 150°C according to a ramp of 10°C per minute (up to 500°C for AN02). The purpose of this heater is to accelerate the evacuation of the water, and to observe the spectral variations associated with it.

1.6. LIMITATION OF THE STUDY

In all site most of the opal mining tunnels are currently abandon because the market value of opals are dropped and most of the tunnels are not giving opal as they were before. So it very difficult to get opal samples directly on the mining sites.

Unlike other gemstone opal has a lot of variety by nature, hence it is difficult to study all types of opal samples and it needs a large number of data and appropriate material resources for laboratory analysis. Therefore this research only concern understand crazing (cracking) phenomenon of white transparent, white translucent and fire opals. So as to perform the study under consideration in accordance with previously submitted project proposal.

In this work the Raman spectral graph only prepared for sample CH01 and KOK04 at room temperature (RT) and 150°C. Files for the other samples are incredibly complicated because there is poor response of opal in the Raman acquisition experimental data it takes long time (even in low resolution) about 12 hours, sometimes 15 hours, to obtain an acceptable signal with the parameters used in this study. In addition, it was observed that the sample could crack during Raman acquisition (under the laser) or after the heating of the exchanged sample. The sample may therefore crack during the Raman acquisition. Therefore I cannot find a consistent data to draw Raman spectra graph. This paper final output is concluded based on characterize under natural light, entre crossed polarizers optical properties and spectroscopic properties at low spectral resolution ($3cm^{-1}$) do not reporting the overall behavior of the samples.

CHAPTER TWO LITERATURE REVIEW

2.1. INTRODUCTION

Opal (chemical formula $SiO_2.nH_2O$) corresponding to a hydrated silica, amorphous or poorly crystallized (Gaillou, 2006). Its water content can vary from 3 to 16% of its weight (Aguilar-Reyes, 2004); hardness is between 5.5-6.5, density can vary from 0.67 for certain hydrophane opals to 2.23 for other varieties (Gaillou, 2006) and its refractive index can vary between 1.42 and 1.475 (Aguilar-Reyes, 2004).

The opal values in the gemological market qualify for its ability to display color schemes and in the industry for its ability to diffracting light in pure spectral colors. This characteristic comes from its internal structure, able to mimic the network of a crystal from an arrangement of "balls" of silica. It can thus diffract visible light. However, the opal tends to destabilize outside of its natural genesis. Once extracted, during cutting and polishing or even well after its sale on the market an opal can present two types of loss of gem quality: either by bleaching or cracking (Rondeau et al., 2011a). The precursors of the synthetic opal also crack when they dry (Filin et al., 2002) as well as industrial inverse opals (Hatton et al., 2010).

2.2. ETHIOPIAN OPAL GENESIS AND STABILITY

There are numerous small deposits of opals around Wegel Tena. All found at a single stratigraphic level and hence all formed at the same time. This layer belongs to a thick sequence of volcanic ash rich in silica called ignimbrites, forming a volcanic tuff (Rondeau et al., 2011b).

The Wegel Tena opal is formed during the Oligocene period (24 to 34 Ma) when volcanic emissions stopped for a long time. This episode had to be long enough to weathering of the host ignimbrite and release the silica. The silica has two origins. The first one is the alteration of feldspars which explained by the abundant presence of potassium, barium and strontium in the opal and the second source of silica is alteration of volcanic glass. Indeed, the percolation of meteoric waters in ashes of ignimbrites can dissolve and mobilize the silica and from a

concentrated solution of silica. This solution fills voids or is trapped in unwelded ignimbrite layers (Rondeau et al., 2012).

The crystallography of opal has controlled, at least in part, the incorporation of chemical impurities may form not well-crystallized opal. That is, although the Wegel Tena opals are poorly crystallized, they consist mostly of tridimensional networks of Si-O bonds (Chamard-Bois, 2015). The variation of opal is due to the silica-rich water did not circulate enough to homogenize the composition, nor to purify it from impurities (Rondeau et al., 2012). However, its properties are consistent with those of opal-CT and most volcanic opals. Inclusions consist of pyrite, barium manganese oxides, and native carbon. Some samples show "digit patterns": interpenetrating play of-color and common opal, resembling fingers (Rondeau et al., 2013). The opaque-to-translucent Wegel Tena opals become transparent when soaked in water, showing a remarkable hydrophane character (Chamard-Bois, 2015).

Many opals have a very beautiful play of colors. However, these gems are often prone to cracking (Filin and Puzynin, 2009). Relatively the fire and crystal opals are prone to cracks, while the white, opaque-to-translucent opals are remarkably durable. The proportion of gem-quality material in the Wegel Tena deposit seems unusually high and 1,500 kg have already been extracted using rudimentary mining techniques. The deposit may extend over several kilometers and could become a major source of gem-quality opal (Rondeau et al., 2012).

Generally, opals are formed by hydrothermal fluid circulation or on pedogenesis of continental weathering from meteoric water. The silica of the host rock is released by the action of water during processing of feldspars and clays volcanic glass, or when the alteration of a clay into another. Silica released in water precipitates in the form of quartz, chalcedony or opal. Opals crystallize in fractures and cavities (Rey, 2013; Rus et al., 2014).

2.3. COLOR SOURCE OF OPAL

Precious opals ("play-of-color" or "noble") can display all the colors of the rainbow in an iridescent, moving pattern of red, green, blue, yellow, purple, aqua, pink, and any other colors. It is more valuable than "common" opals, which do not display this optical phenomenon. The play-of-color is due to diffraction of visible light on a perfect network of silica spheres having

the adequate diameter, between 150 and 300 nm described by Sanders (1964). Common opals can still be very valuable as gems for their transparency and their body color which spans a large spectrum (Gaillou et al., 2008).

The concentrations of the main impurities in opal which are greater than 500 ppm are Al, Ca, Fe, K, Na, and Mg. Other impurities may be present Such as Ba, Zr, Sr, Rb, U, Y, Pb, Mn, Zn and Cu. Some of these elements may have an impact on the physical properties of opals. Even in low concentrations, for example: - uranium luminescence of green color, the presence of iron in fire opals is responsible for the intensity of the color orange. The whole of these impurities may or may not be present in the opals and in varying amounts. They are very often representative of the chemical composition of rock (Fritsch et al., 1999; Gaillou et al., 2008; Chamard-Bois, 2015). In general the body color in the opal mass is due to the presence of colored mineral inclusions (Chamard-Bois, 2015).

2.4. OPAL-A AND OPAL-CT

2.4.1. Structure of opal-CT

According to Elzea and Rice (1996) the structure of opal-CT analyzed by X-ray diffraction (XRD) examination demonstrate that opal-CT corresponds to a poorly crystallized silica composed at the atomic level of a continuous series of intergrowths of polymorphic phases α -cristobalite and of α -tridymite stacking sequences. Tridymite is believed to correspond to a layer in the cristobalite which shows stacking fault tetrahedra SiO_4.

2.4.2. Amorphous opal (opal A)

Opal is amorphous (cryptocrystalline) regarding the crystal system. Characterized by a highly disordered almost amorphous material similar to glass; it may have a structure without arrangement (Jones and Segnit, 1971).

2.5. HYDROPHANE CHARACTERISTICS OF OPALS

The term hydrophane is defined for translucent opal having a dull appearance and opaque in the air. However, when immersed in water they become shine and transparent colorless. This phenomenon is totally reversible. That is why they return to their original appearance when

they drying (Chamard-Bois, 2015). These opals adhere on tongue and fingers by capillary action. Also the weight increases when the opal is immersed into water for a while (Rondeau et al., 2011a).

2.6. WATER IN OPALS

Water in opals exists in two forms: silanols (Si-OH groups) and water molecular H_2O. There are several types of molecular water in the opal: it can be trapped in the structure of the opal form of isolated molecules (Gaillou, 2006); form Fluid inclusions; or adsorbed on the inner surfaces of the opal (Aguilar-Reyes, 2004). Silanols exist in the internal defects of silica, as well as on internal surfaces as external to the opal, where they are capable of forming hydrogen bonds with molecular water, which allows its adsorption (Gaillou, 2006).

Segnit et al. (1965), occurrence of water in natural opaline silica has been studied by differential thermal analysis, thermo gravimetric analysis, infra-red analysis and nuclear magnetic resonance. The results show that in the "crystalline" opals 90% or more of the total water is physically adsorbed whereas in "amorphous" opals at least 20% but perhaps much more of the total water is held as hydroxyl groups chemically bonded to the silica surface.

2.7. DESTABILIZATION

When opal is mined the samples often appear as nice pieces that seem to promise beautiful cut samples. After a while, some rough samples destabilize either by cracking or whitening, a phenomenon often referred to as “crazing”: it can occur within a few hours after mining or even sometimes after several months. It can also happen during or after being cut and polished (Rondeau et al., 2011a).

This destabilization phenomenon is unpredictable over time and there is no direct method to predict which sample will destabilize and which other will not. In effect, there are only major trends observed in deposits, which are not always true. No correlation was found between observable physical parameters (like density and refractive index) and the susceptibility of destabilization (Pearson, 1985).

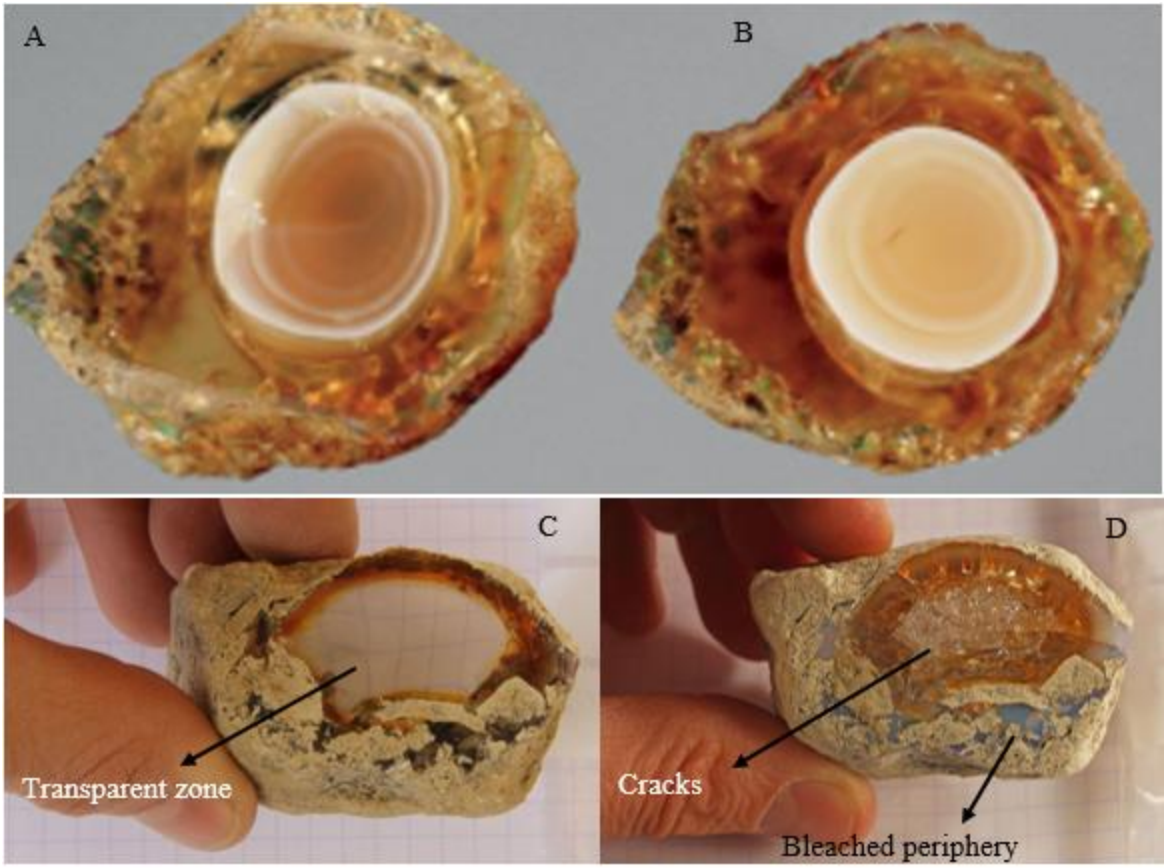

Figure 2.1: **A)** and **B**) orange opal (24 g total weight) from Wegel Tena were sliced to show the internal 15-mm diameter egg-shaped zone of destabilization Photo by B. Rondeau (Rondeau et al., 2011a). **C)** A transparent opal photo captured in 2013 **D)** the photo of sample C preserved in room temperature till 2016 for 3 years and shows a lot of crack patterns and peripheral bleached zone, opal from the province of Wello, Ethiopia. (Photo: B. Rondeau)

2.7.1. Cracking of opal

According to Rondeau et al. (2011a) Crack destabilization consists of the appearance of a network of cracks through the gem (Figure 2.1). This cracking may occur just after the gemstone is extracted, a days, months even years later. Cracking occurs in all varieties of opal, but is most common in truly amorphous opals (opal A).

Cracking may manifest itself as a network of cracks and can develop throughout the sample, or remain near its surface. More rarely, cracks develop inside the opal. It is best seen in transparent opals, although it can occur in translucent and opaque ones as well. This makes

the opal much more fragile, brittle and in most cases it becomes unsuitable for mounting in a piece of jewelry. The phenomenon can also occur when cutting or polishing the gem. In general, these cracks remain close to the surface or cross the gem. However, they may also rarely grow only at the center of it. Cracking only begins when the opal is dried and exposed to air (Rondeau et al., 2011a).

One common accepted tendency is that destabilization is related to a change in the water content of the opal (Pearson, 1985; Aguilar-Reyes, 2004; Rondeau et al., 2011a).
The role of water has been examined by Pearson (1985) most often destabilization is attributed to loss of water but few measurements exist. Some believe that plunging a destabilized opal in water stabilizes this opal. In fact, this experiment only drives water into the cracks, making them less apparent. This is somewhat like impregnation. The opal is not cured, and if left to dry, cracks or whitish volumes will appear again. Smith (1988) relates two methods, both based on controlled drying (hence related to water) to cure apportion of Oregon opal that is in the process of crazing. Virgin Valley (Nevada) miners reported to one of the authors (EF) similar results with sparse unpredictable success. This unfortunate effect is associated with appreciable water content in the open pores of the material. Internal stresses arise upon any dehydration resulting in surface shrinkage and progressive cracking (Filin and Puzynin, 2009).

Aguilar-Reyes (2004) studied destabilized opals (whitening) from Mexico, Honduras, and Ethiopia (Shewa province at the time). She measured water loss and specified surface accessible through open porosity comparing the stable parts of the opal samples with their destabilized portions. She demonstrated that in the majority of cases (13 out of 17) destabilized opal loses water. The degree of water loss varies from 48 to 95 percent (Aguilar-Reyes, 2004; Aguilar-Reyes et al., 2005).

Opals from Wegel Tena deposit in the province of Wollo Ethiopia is exploited for opals noble gem quality since 2008 (Rondeau et al., 2011b). These have a very beautiful play of colors. However, these gems are often prone to cracking only with the course of time or just mild heating. This unfortunate effect is associated with appreciable water content in the open pores of the material. Internal stresses arise upon any dehydration resulting in surface shrinkage and progressive crazing and cracking. These defects make many Ethiopian opals unsuitable for

use in jewelry (Filin and Puzynin, 2009). This is an economic problem for the exploitation of this deposit. Indeed, it is estimated that 5% of Wegel Tena opals cracking from the first cut to size the rest can crack later (Rondeau et al., 2010).

2.8. BIREFRINGENCE

Gem minerals belongs into two optical classes, isotropic (single refracting index) a ray of light which enters isotropic substance regardless of the direction in which the ray enters the gem will obey Snell's law of refraction and will produce a single refracted ray. While Anisotropic (double refracting) a ray of light which enters an anisotropic substance is not only bent or refracted, but it is also broken or split into two rays, each of which travels with a different velocity and hence has a different refractive index (Strubbe et al., 2015).

Amorphous materials (glass, opal and amber which lack a regular internal structure), as well as gemstones belongs to the cubic system (diamond, garnet, spinel, fluorite etc...), they are all defined by a single refractive index (isotropic), since light is propagated with equal velocity in all directions within the material (Howell et al., 2010).

Imaging isotropic material between crossed polarizers shows only single refractive index and no birefringence. Possession of more than one index of refraction between crossed polarizers shows birefringence, the greater the difference between these indices, the greater the birefringence. The ray with the lower index of refraction is called the fast ray. The ray with the higher index of refraction is called the slow ray. The difference in the indices of refraction between the fast and slow ray $\delta = ns - nf$ is called birefringence (Howell, 2012).

The occurrence of birefringence in cubic mineral is an anomalous optical property, which is the result of the photoelastic effect producing a change of refractive index with stress (Nye, 1957 and Poindexter, 1955). Howell (2012) observes birefringence pattern when he imaging a diamond crystal between crossed polarizers which later helps him to learn about its history of deformation and the possible cause of change of refractive index with stress.

For centuries scientists have been postulated several possible sources of abnormal birefringence in isotropic minerals and natural amorphous materials. 1) Lang (1967) states that, mineral inclusions are one of the major causes for the existence of abnormal

birefringence in diamond crystal which is a result of lattice closure errors in the host diamond (host mineral). 2) Howell et al. (2010) describes that, the mineral inclusion, would generate dislocations in the host mineral which were the cause of the resultant birefringence. 3) Rosenfeld and Chase (1961) come up with a conclusion that, the mineral inclusion and its host mineral's differences in coefficients of thermal expansion and compressibility would cause optically anisotropic strain effects around the inclusion and they states that, this could be another possible cause to produce interference pattern around the strain.

2.9. SPECTROSCOPIC PROPERTIES OF OPALS

A first model that allows making the link between micro-constraints and Raman spectroscopy was proposed by Ganesan et al. (1970). It relates the constraints internal sources of material, deformation sources in atomic bonds and a shift between the Raman peaks of stressed and resting material. A deformation of the order of 1% causes a shift of the order of $10cm^{-1}$. Studies on crystalline silicon show a shift towards the high numbers of waves in the presence of compressive stresses and to low wave number in the presence of extensive constraints (Strubbe et al., 2015).

On amorphous silicon hydrate the same shifts are observed, but the isotropic aspect of the amorphous material does not make it possible to differentiate uniaxial, biaxial or triaxial (Strubbe et al., 2015).

Tallant et al. (1988) studied the effect of extensive stresses on silica glass, that can be considered here as a very good proxy for the opal (Figure 2.2), because of the proximity of the Raman spectra of these materials. They showed a negative shift from 17 to 39 cm^{-1} for peaks at 440, 800, 1050 and 1190 cm^{-1}, and a few cm^{-1} for peaks at 490 and 605 cm^{-1}. The applied extensive stress was 10.3 GPa (Figure 2.2). The variation in peaks at 440 and 800 cm^{-1} is associated with an angular deformation of the Si-O-Si. Variation peaks at 490 and 605 cm^{-1} is linked to a deformation of rings of three or four tetrahedra SiO_4. The variation peaks at 1050 and 1190 cm^{-1} is unexplained by these authors. The unconstrained opal-CT shows Raman peaks at 314, 343, 406, 478, 569, 646, 780, 803, 909, 948, 1050, 1072, 1139, 1197, and 2899 cm^{-1}. A massif is centered between 325 and 328 cm^{-1} (Figure 2.2). Cristobalite contributes to the spectrum with peaks at 403, 412, 460 and $512cm^{-1}$ (Chamard-Bois, 2015). Molecular

water is observed between 3300 and 3500 cm^{-1}, and the OH groups between 3600 and 3650 cm^{-1} (Behrens et al., 2006).

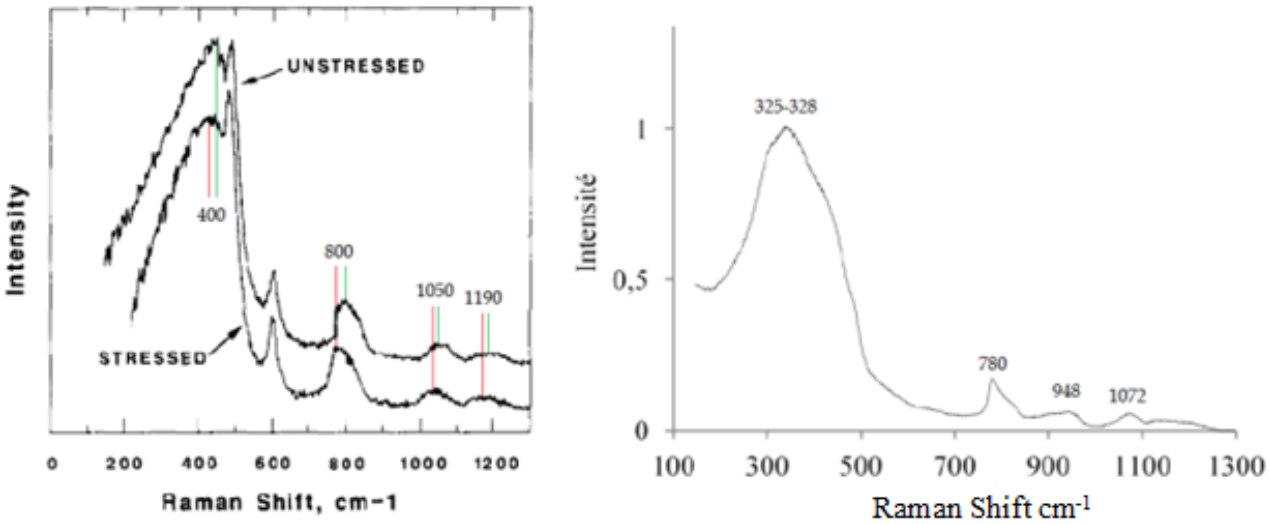

Figure 2.2 -Left, Raman spectrum of amorphous silica, strained extensive guide (peaks marked in red) and unconstrained (peaks indicated in green). Modified from Tallant et al. (1988). **Right**, Raman spectrum of opal-CT from Wegel Tena. The spectra are of the same shape but slightly shifted. Modified from Chamard-Bois (2015).

2.9.1. Raman spectroscopy of opals-CT

The CT opals present on their Raman spectrum a massive centered between 325 and 328 cm^{-1}. The Shoulders at 403, 412, 460 and 512 cm^{-1} are caused by cristobalite. It is also possible to find contributions from quartz and tridymite. The strips are generally wide because structure of the opals is very poorly crystallized. The mass towards 3215 cm-1 corresponds to the molecular water (Ostroumov et al., 1999). The set of peaks present on the Raman spectra of CT opals associated with their physical phenomenon is listed in table 2.1 below.

Number of waves (average)	Physical phenomenon (s)
325 and 328cm^{-1}	Semi crystalline opal (Opal-CT) (Kiefert and Karampelas, 2011).
343 cm^{-1}	- O-Si-O angular vibrations in 6-membered SiO rings (Ivanov et al., 2004) - Contribution of trydimite (Wilson, 2014)
406 cm^{-1}	Quartz phase or Si-O-Si angular deformation (Aguilar-Reyes, 2004)
478 cm^{-1}	-Vibrations of the rings of 3 or 4 members (Aguilar-Reyes, 2004) - T - O - T angular deformation with T = Si, Al (Behrens et al., 2006)
569 cm^{-1}	Vibrations of 1 to 3-member rings containing one or more Al (Lelosq et al., 2014)
646 cm^{-1}	Intensity proportional to the brown color (Gauthier et al., 2004)
780 cm^{-1}	- Symmetrical elongation Si - O - Si for rings of 3 or 4 Members (Smallwood,2000)
803 cm^{-1}	Ring structures (Rossano and Mysen,2013)
909 cm^{-1*}	Antisymmetric elongation Si - O in Q^1 (Rossano and Mysen,2013)
948 cm^{-1}	Antisymmetric elongation in Q^2 (Rossano and Mysen,2013)
1050 cm^{-1*}	T2 vibration mode in TO_4 tetrahedra (Lelosq and Neuville, 2013)
1072 cm^{-1*}	- Symmetric elongation Si - O - Si (Smallwood,2000) - Vibrations involving oxygen bridging in units Which do not need to be fully polymerized or Vibrations of Si - O associated with alkaline earths or of metallic alkalis (Lelosq and Neuville, 2013) - Raman spectra quartz and trydimite have a peak at 1075 cm-1 - Q^3 (Rossano and Mysen,2013)
1139 cm^{-1*}	T - O elongation (Behrens et al., 2006) Q4 (Lelosq and Neuville, 2013)
1197 cm^{-1*}	- Q^4 (Lelosq and Neuville, 2013; Lelosq et al., 2014). - Environment of Q^4 different from Q4 to 1139 cm-1.

2899 cm^{-1*}	Band present in the natural cristobalite formed by recrystallization of Silica glass (Smallwood,2000)
3000 – 3500cm^{-1}	H_2O molecules (Smallwood,2000)
3500 – 3600cm^{-1}	OH Groupings (Smallwood,2000)

Table 2.1: Position of peaks on the Raman spectrum of the opals and associated physical phenomenon. The interpretation of the peaks followed by a * is controversial in the literature after the work of Chamard-Bois (2015).

CHAPTER THREE GEOLOGICAL SETTING

3.1. REGIONAL GEOLOGY

The existing geological map of Ethiopia show that the country is covered by 18% Precambrian basement rock, 25% Mesozoic sedimentary rock and 56% Cenozoic volcanics and sediments (Solomon, 2000).

Precambrian basement exposures are found in areas which are not affected by intensive Cenozoic volcanism, rifting process and the place where Mesozoic cover has been eroded away. The Precambrian rocks exposed in four major areas of the country in North (Tigray region); West (Gojam,Wollega, Illibabore and Kefa); East (Harerghe region) and South (Sidamo and Bale). In the Precambrian basement two lithostratigraphic assemblages have been recognized these are gneissic terrains found mostly in the Southern sector of the country and metamorphosed volcano sedimentary belt mostly dominate in the Northern sector of the country (Kazmin, 1972).

According to Kazmin (1972), the Ethiopian late Paleozoic to Mesozoic sedimentary formation was deposited in related to transgression-regression cycle. Mengesha et al. (1996) described the first transgression started in the early Jurassic to Late Triassic and forms the Ogaden region in the Southeast to towards Northwest and reached its maximum extent in Kinmeridgian. During this time Adigrat formation, Hamanilei formation and Abay formation were deposited. Regression of the sea started towards the end of Jurassic depositing Lagoonal Facies of Agula formation. The lower most cretaceous is represented by the Korahe formation in the Ogaden region and marks the first regression event. The second regression transgression event took place in Aptian and Turonian depositing Mustahil formation, Ferefer formation and Belet formation. In the late cretaceous the second regression event took place and depositing continental sediments in the country.

The mid tertiary (~ 30 Ma) Ethiopian continental flood basalt form part of the large Afro-Arabian igneous province, which is related to the Afar plum and Red sea-Gulf of Aden Ethiopian Rift triple junction (Kurkura, 2010). The Ethiopian volcanic province is composed of a Tertiary Basaltic pile, with thickness varying from 700 to 2000m. It covers an area

several hundred kilometers across on the plateau on either side of the main Ethiopian rift Afar depression (Berhe et al., 1987).

3.1.1. The Cenozoic Ethiopian plateau volcanic province

The Ethiopian plateau form the largest part of extensive continental flood basalt province which resulted from mantel plume-head activity associated with the opening of the Red Sea and Gulf of Aden at the Afro Arabian triple junction (Marc et al., 2003?). The tertiary volcanism in Ethiopia has persisted for at least 45 million years (George and Rogers, 2002).

Mohr (1962) divide the Cenozoic volcanic rock of Ethiopia in to Trap and Aden series. Trap series used to refer the whole pile of the tertiary flood basalt sequence with intercalations of felsic lava and pyroclastic rock which forms south western and south eastern plateau. The term Aden series used for post rift (middle Miocene to quaternary) volcanic rock of the main Ethiopian rift, Afar Depression and some part of Ethiopian plateau.

The flood basalt and other subordinate volcanism in Ethiopia during tertiary time has built up a sub areal volcanic pile having a thickness range from 500-1500m and locally attain a thickness of 3000m (Mohr and Zanettin, 1988). The Ethiopian continental flood basalt has an estimated total areal coverage of 600,000km^2 and not less than 750,000km^2 before erosion (Mohr, 1963; Mohr and Zanettin, 1988). And the preserved volume of the province has been estimated 350,00km^3 (Baker et al., 1972). Tertiary flood basalt and their intercalated silicic volcanic now uplifted on the western and eastern (Harar) plateau of Ethiopia and cover an estimated volume of about 300,000km^3**.** The flood basalts of the Ethiopian Traps are transitional between tholeiitic and alkaline in composition (Mark et al., 2003?).

3.1.1.1. Northwestern Ethiopian plateau volcanic province

Northwestern Ethiopian continental flood basalts (CFBs) preserve a record of magmas generated from the center to the flanks of a plume head, currently corresponding to the 'Afar hotspot'. Basaltic lavas appear zonally arranged with Low-Ti tholeiites (LT) in the west, High-Ti tholeiites (HT1) to the east and very High-Ti transitional basalts and picrites (HT2, TiO_2 4-6 wt. %) closer to the afar triple junction (Luigi et al., 2009). In this province, up to 2 km thick predominantly mafic lavas with minor felsic pyroclastic make up the northern part of

the Ethiopian flood basalt sequence e.g., (Hofmann, 1997; Ayalew et al.,2002) and cover an area of ~ 106 km^3 (Rochette et al., 1998; Kurkura, 2010).

The Ethiopian continental flood basalt is characterized by the presence of large volume felsic volcanic rocks (>$6\times10^4 km^3$) with overall thickness not more than 700m, covering and interlayering the upper part of the basaltic sequence (Ayalew and Yirgu ,2003).

Ayalew et al. (2002) recognized three different plateau rhyolite units. (1), Lima Limo rhyolites, outcropping in the northwestern sector of the northern plateau having TiO_2 between 0.25 and 0.45% and interbedded with low-TiO_2 flood basalts; (2) Wegel Tena rhyolites TiO_2 between 0.45 and 1% deposited in the eastern sector nearer the Afar rift margin overlying high-TiO_2 basalts; (3) Jimma rhyolites TiO_2 between 0.45 and 0.72% found in the southwestern Ethiopian plateau capping high-TiO_2 flood basalts. The Wegel Tena ignimbrite exhibit dominantly porphyritic texture with common Phenocryst assemblage of sanidine and anorthoclase, quartz, clinopyroxene, amphibole and ilmenite set in a glassy or fine-grained groundmass.

The existence of both basalt and rhyolitic rocks in the same province suggest that the rhyolitic rocks are a result of extensive fractional crystallization and varying amount of crustal contamination of the exposed basaltic magma (Ayalew and Yirgu, 2003). The petrological and geochemical characteristics of the plateau basalt show consistency with it derivation from fractional crystallization of basaltic magmas similar in composition to the exposed flood basalts (Ayalew et al., 2002). The earliest volcanism in south western Ethiopia the Akobo basalt gives an age of 45.4 Ma (Berhe et al., 1987).

In general Mengesha et al. (1996) classify the major Cenozoic volcanic cover of the northern Ethiopian plateau sector in to the following unit. Ashnghi formation it represent the earliest fissural flood basalt vocanism in the North Western plateau which represent thick of strongly weathered crushed tilted basalts which lies below pre-Oligocene unconformity (Zanettin et al., 1980).

The Ashenghi formation predominantly consists of mildy alkaline basalts with interbeded pyroclasts and rare rhyolites. It is believed that Ashanghi formation is restricted in the North Western plateau until a group of flood basalts were found in South Western Ethiopian plateau

(Davidson, 1983) with K/Ar age range between 49 to 36 Ma like Akobo basalt 49-46 Ma and now considered to be analogous with basalts of the Ashanghi formation (Mengesha et al., 1996).

Aiba Basalt they are generally aphyric, compact rock in place showing stratification and contain rare interbedded basic tuffs (Mengesha et al., 1996). The basalt shows distinctive tholeiitic nature with transition to mildly alkaline varieties. The absolute age of the Aibs basalts range from 34 to 28 Ma placing them in Oligocene (Zanettin et al., 1980).

Alajea formation mainly consists of aphyric flood basalts associated with rhyolitic (ignimbrites) and subordinate trachytes. These formation ranges in age between 36 to13 Ma. The Alajea formation contains transitional to tholeiitic in nature and an increase in alkalinity is observed in the younger member of the formation (Mengesha et al., 1996).

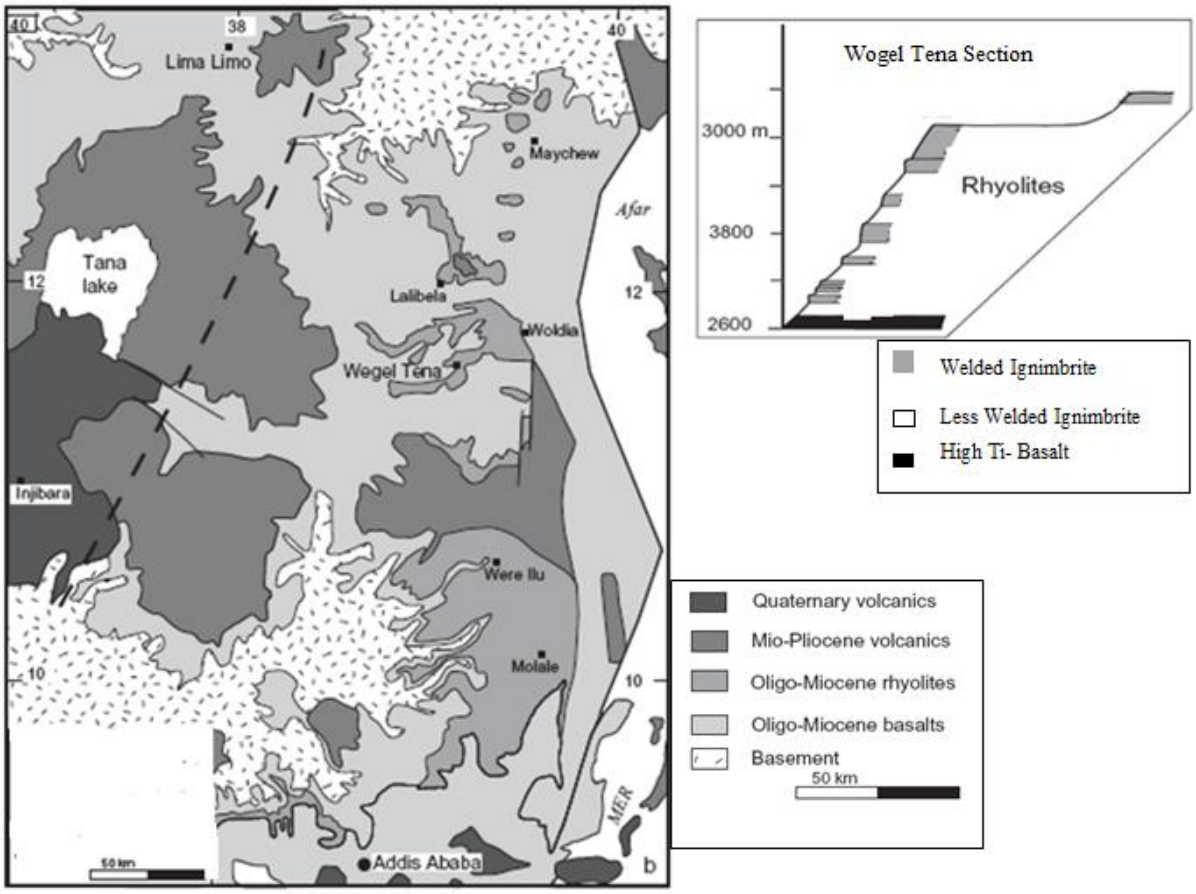

Figure.3.1: Location map of northern Ethiopian Plateau volcanic province, Afar Rift and Main Ethiopian Rift (after Merla et al., 1979). The approximate broken line separates the low-Ti and High-Ti flood basalt province of Pik et al. (1998) with stratigraphic profiles of Wegel Tena sections after the work of Ayalew and Yirgu (2003).

3.1.1.2. Southeastern Ethiopian plateau volcanic province

Except some regional geologic, petrologic and geochronology study, detail geological studies are lack in the Southeastern Ethiopian plateau volcanic province. Berhe et al. (1987) classified the Bale (south eastern Ethiopia) Cenozoic volcanics in to four major groups forming a succession of Basalt and Trachyte: the Lower Stratoid Basalts, the Reira Basalts, the Dodola and Aroresa Trachyte and the Senta Basalt and Batu Trachytes.

600m thick upper Miocene flood basalts (Reira Basalts? 15-5.3Ma) cover the Batu Mountains region where they rest directly on the older flood basalts (Mohr and Zanettin, 1988). In

contrast with this older aphyric basalts the younger one include both plagioclase and pyroxene phyric type and the flow are frequently scoriaceous and separated by paleosols (Berhe et al., 1987; Mohr and Zanettin, 1988).

Berhe, et al. (1987) grouped the Cenozoic volcanisms of Bale (southeastern Ethiopia) area into four major groups forming a succession of basalt and trachytes about 2000-2300m thick. (1), Lower stratoid basalt 10-150m thick of weathered ahpyric basalt which directly rest on the protrozoic basement.(2), The Reira basalt which form 600m succession of ahpyric, pyroxene and plagioclase-aphyric basalt. The Reira basalt is unconformably overlain by the Aroresa trachytes and Dodola ignimbrites which is restricted to the Northwest. (3), The Dodola and Aroresa trachytes, the Dodola ignimbrites primarily composed of rhyolitc ignimbrites trachytes and ash flow tuffs. (4), And the Sanete basalt and Batu trachytes which form the second highest volcanic edifices in Ethiopia. This volcanic were erupted from different centers and display rapid lateral thickness variations.

3.2. GEOLOGY OF THE STUDY AREA

3.2.1. Introduction

The Cenozoic volcanic rocks of the study area are mostly dominated by basaltic lava flow and pyroclastic deposit (ignimbrite). The lower parts of the volcanic sequences in the area dominated by basaltic rocks, found to be gentle slope forming undulating topography with high degree of weathering, on the contrary basalts on the upper parts form steep cliff in some places with columnar jointing structures overlying the lower basalts and in some place on the rhyolitic ignimbrite parts of the area.

In the area rhyolitic ignimbrite rock have a total thickness ranging from 400m to 700m around Chege area (Chege is one of the best opal artisanal mining site in Delanta woreda). The rhyolitic ignimbrite rocks have an alternative layer of welded and unwelded pyroclastic flow (Ignimbrite). The lowest elevation is 2900m a.s.l which is recorded around Chegen River where the artisanal mining activity takes place.

Detail geological and petrological examinations of the Cenozoic volcanic rocks of the area are discussed below.

3.2.2. Rhyolitic Ignimbrite

Ignimbrite (pyroclastic flow) unit of the area has rhyolitic composition. The unit is the host rock for opal resource of the study area with varying physical property in different places (Detail description of the opal host rock of the area is discussed below). This rock unit in the area has a thickness varying from 400-700m. The units exposed in the central and eastern part of the study area. North of Wegel Tena town it is extensively eroded and dissected by the deep gorges forming sharp cliffs. Along Wegel Tena-Beshsilo river road section it forms plains.

The rock is pink, white, light gray and fine to coarse grained. The unit is layered or bedded and individual flows vary in thickness < 3m up to 15m. The individual layers show variation in texture, they are dominantly porphyritic with glassy matrix. Densely welded ignimbrites

have a glassy appearance and exhibit a well-developed columnar jointing structure mostly on the upper parts of the succession.

Along the river of Chegen this rock exposure is extensive and the lower contact with other unit is not visible, following this river in some areas the exposure is not even reach to the layer of opal host unit. In different places and different altitude the unit shows variation in degree of weldness and lithic fragment proportion. Around Chegen locality (northwest of Wegel Tena town) at elevation of 2949±6m a 20m thick layer of ignimbrite shows very high welded and glassy nature.

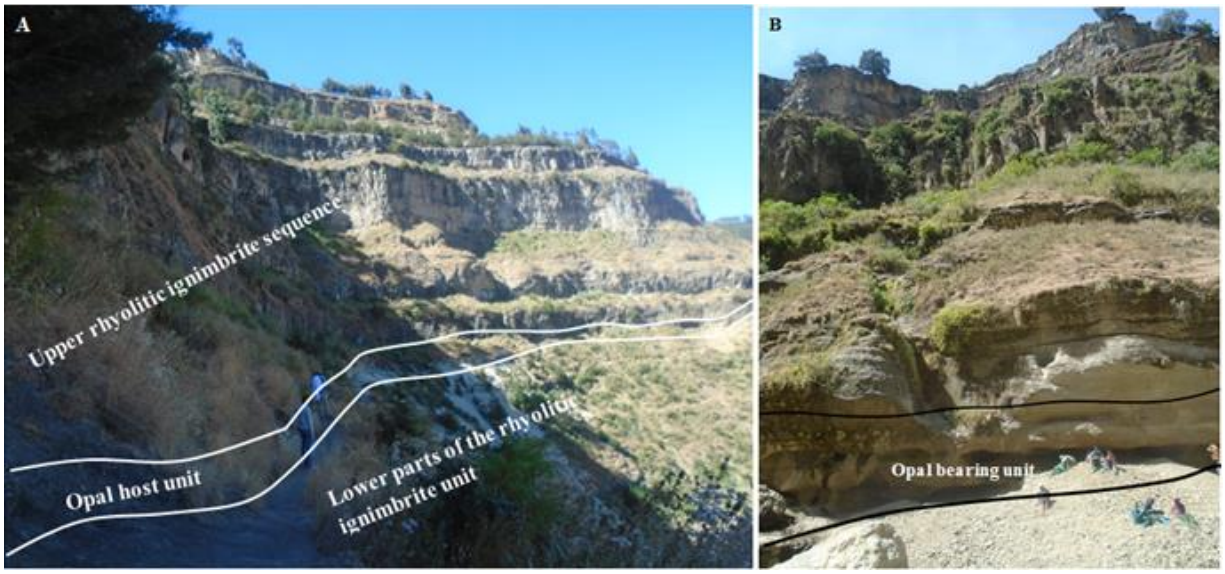

Figure 3.2: A), General lithostratigraphy of the study area (photo from Koke Wuha locality) showing the lower parts of the rhyolitic ignimbrite sequences having gentle slope with high degree of weathering; and the upper parts of the sequence form steep cliff with alternating layer of rhyolitic ignimbrite (both welded and unwelded), and at the middle a very thin layer, not more than 3m thick lithostratigraphic position of opal bearing zone. **B)** Photo of a closer look of highly unwelded opal bearing rhyolitic ignimbrite at Anset locality mining site with the local artisanal miner at work.

Figure 3.3: Photos taken from Chegen locality around 17km north of Wegel Tena town showing the variation of topographic slopes, the top part steep slope cliff is formed by Highly welded ignimbrite; and lower part relatively gentle slope topography is formed by unwelded ignimbrite, the steep slope lithology at the top of the sequence (welded ignimbrite) relatively has a resistance to any kind of weathering that is why it forms steep slope relative to the unwelded one (bottom part).

3.2.3. Basalt

In the area two different types of basaltic lava flow units are exposed. Lower basalt which is the lower volcanic succession of the area with a thickness varies between 500 to 700m. And vesicular basalt, this unit in most parts of the area overlies the lower basalt in a place where the rhyolitic ignimbrite unit of the area are absent or eroded away.

In the area the lower basalt unit is exposed dominantly in the central, southern tip and to the western parts following river cuts. These basalts represent the earliest fissural volcanism in the area (Tefera et al., 1996). These basalt flows represent the lower most parts of volcanic successions. They are exposed along the deep river gorges in some parts of the area. The unit is exposed along road cuts, stream beds, gentle and steep slopes of undulating mountain chains and low lying flat plains. Its lower contact with the underlying unit is not seen in the area. The unit is unconformably overlain by the rhyolitic ignimbrite and vesicular basalt formation. Their contact with the rhyolitic ignimbrite is clearly observed on Wegel Tena area. Megascopically the rock is black, dark gray and greenish gray in color. Texturally it varies

from aphantic, porphyritic to sub-porphyritic. It has greenish alteration zones seen along the fracture zones, in the pyroclasts and along its contact with the overlying rhyolite.

The second basalts of the area vesicular basalt exposed dominantly to the northern portion of the area. It is exposed by forming chain of ridges, cliffs along the escarpment and river cuts and tributary streams. This unit dominantly underlines by the lower basalt of the area and in some parts of the area it underlies by rhyolitic ignimbrite unit. Dominantly the unit has vesicular texture with minor aphantic to sub porphyritic texture basaltic lava flow.

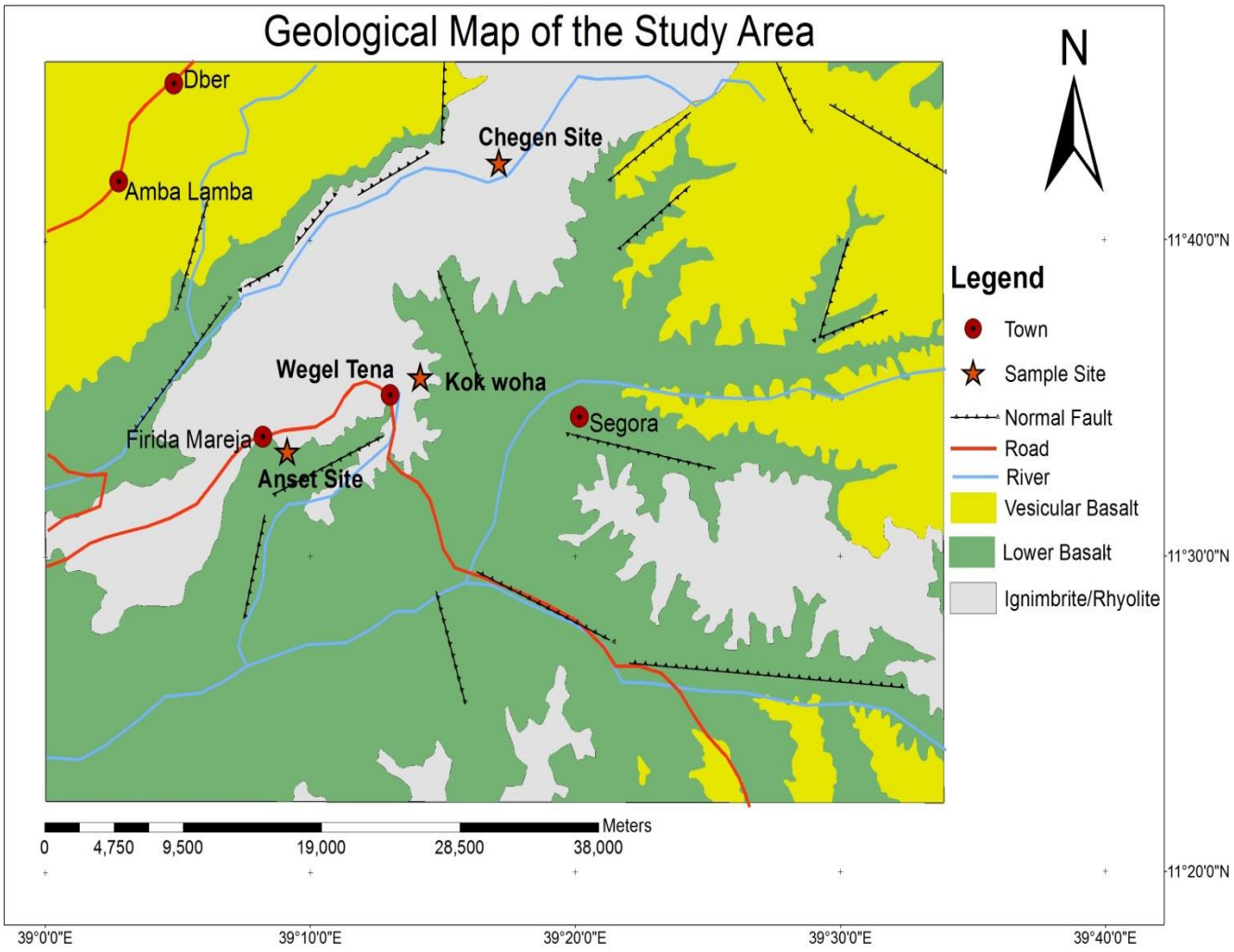

Figure 3.4: Geological map of the area showing, lithological distribution, Sample site location and major fault escarpments. The Northwestern and central parts of the map is prepared in this work and Southern and Eastern tip of the area is prepared by a data obtained from Geological survey of Ethiopia (Tesfaye et al., 2010; unpublished report).

3.3. GEOLOGY AND PETROGRAPHY OF THE OPAL HOST ROCK

3.3.1. Geology

The Wegel Tena opal deposit found in the Ethiopian traps series volcano-sedimentary layers of rhyolitic ignimbrites, set up in Oligocene consisting of several small deposits (Mazzero et al., 2010). The host ignimbrites layer consists of lateralized massive strata with columnar flows and thin poorly consolidated tuff strata. The Wegel Tena opals were formed during the pedogenesis of poorly consolidated ignimbrites, by mechanical alteration of feldspars and volcanic glass. The soil which is rich in argillaceous cavities traps water, allowed recrystallization of silica opal (Chamard-Bois, 2015)

Wegel Tena's opals are often hydrophane, white and translucent fire opals (Rondeau et al., 2010). They are type of opal- CT. One of the major economic problems of Wegel Tena opal deposit is the properties of bleaching and cracking after they are mined from their natural place of genesis (Rondeau et al., 2011a). Indeed, it is estimated to be 5% of the opal crack from the first cut to size (Rondeau et al., 2010), the rest can crack later.

The opal bearing rock unit in the area is rhyolitic ignimbrite bed which has not more than 3m thickness. Within the 3 meter rhyolitic ignimbrite bed there is three different opal host thin layers. The three thin opal host rhyolitic ignimbrite layers separated by very thin layers of fine and equal grain size ash layers (tuff), the local artisanal miners call it “Mekenet” which means a tie between. According to the local artisanal miners the opal quality which is mined from the lower thin layer has low quality and low market value (mostly they are transparent opal with very low play of color). The middle opal host ignimbrite layer gives opal with high play of color, in this layer because the size of the opal is small (1cm to 2cm) there market value is medium. The best quality opal (with respect to play of color, size and stability) in the area is mined from the upper part of the 2 meter ignimbrite bed.

The local artisanal miner testify that, the opal which is mined from the area has three different grads based on their stability, play of color and size but there grade is only on the bases of the market value of the opal.

1. Large size opal with high play of color, in the current market this opal have 100-200 birr per gram value. The local miner call this opal "CHRISTIAN OPAL" (They told us because this opal never crack and never show any whitening how long it expose to the air this is the material you can rely on and this is the property never let you down just like a Christian person).

Figure 3.5: A) Large size opal with high play of color; the local miner calls it "CHRISTIAN OPAL''; **B)** Small size with medium play of color opal, local miner call it "AJARA'' which

means not much; **C)** Small to large size with no play of color, transparent to translucent. Local miners call it “GIM OPAL” which means worthless.

2. Small size with medium play of color, they call it “AJARA” which means not much (this opal category have low market value). The opal is mined from the middle part of the opal host rhyolitic ignimbrite layer. Even if the size of the opal grain is small (1cm to 2cm) they have a play of color with high stability.
3. Small to large size with no play of color, transparent to translucent. They call this opal “GIM OPAL” which means worthless. This opal has no market value because after it is extracted and exposed to air within a second it develops a set of cracks and loses its transparency quickly.

Figure 3.6: a typical viewpoint onto Anset Locality to West of Wegel Tena Town, the opal bearing unit and local artisanal mining sites can be found around 500m below.

3.3.2. Petrography of Opal Host rock

The samples obtained for the petrographic study are from three different sites (Koke Wuha, Anset and Chegen sites where local artisanal mining activity are held). During sampling the samples were taken from the mining tunnel to obtain the least altered and representative samples. Wherever possible the samples are taken with opal crystal to show the growth of opal in the rock. The host rocks are a 3m thick rhyolitic ignimbrite with a tin alternating layer of fine and equal grain size ash layers (tuff).

In hand specimen the rocks are gray in color and fine to medium texture containing large white non transparent opal crystal (W-1, W-2, W-3, W-4 and W-5) and transparent opal with play of color (W-6).

Random anhedral crystal of plagioclase feldspars, Radial-fibrous Chalcedony, anhedral Quartz crystal and small proportion of anhedral pyroxene, Sanidine, Hornblende, lithic-fragment and Opaque (Fe-oxide) with >70% volcanic glassy material form the frame work of this rock mass. The interstices material composed of large proportion of Volcanic glass, Chalcedony, pyroxene and opaque mineral (Fe-oxide) which fills large crystal of Plagioclase, quartz and Chalcedony crystals dominantly. The mineral modal proportion of all rock samples are summarized below in table 3.1.

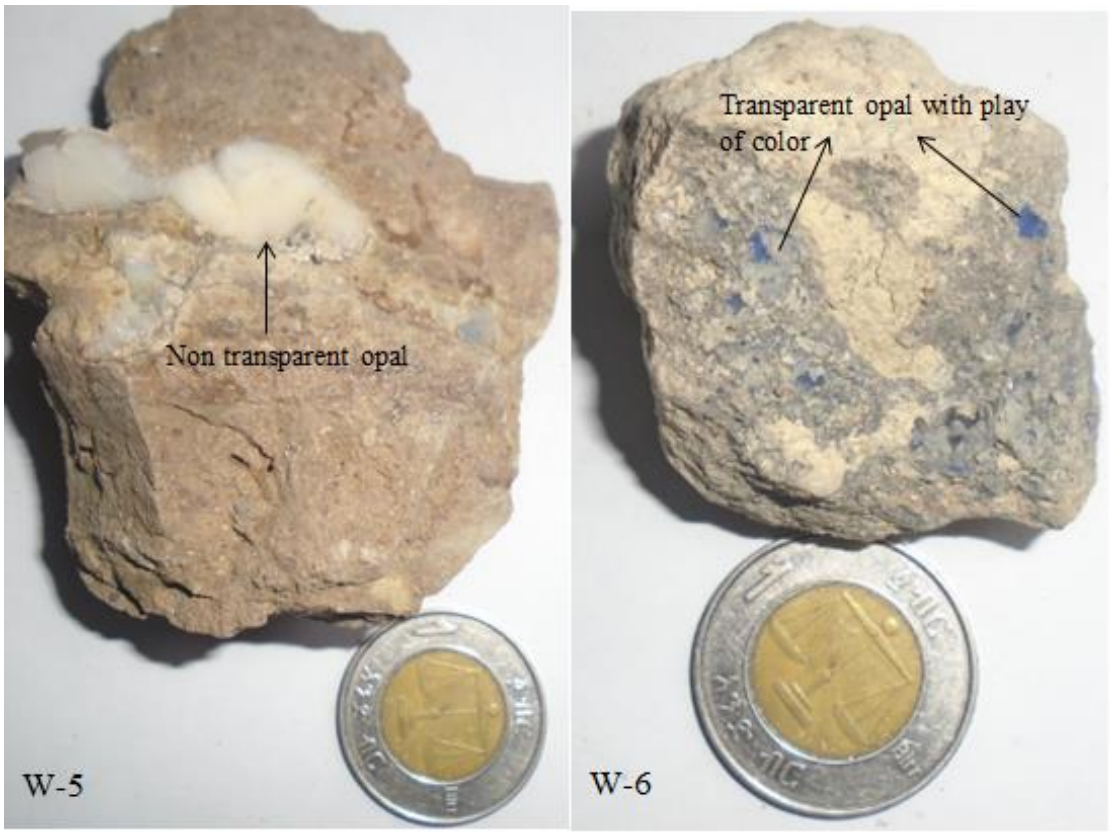

Figure 3.7: Rock samples with white non transparent opal crystal (W-5) and transparent opal with play of color (W-6).

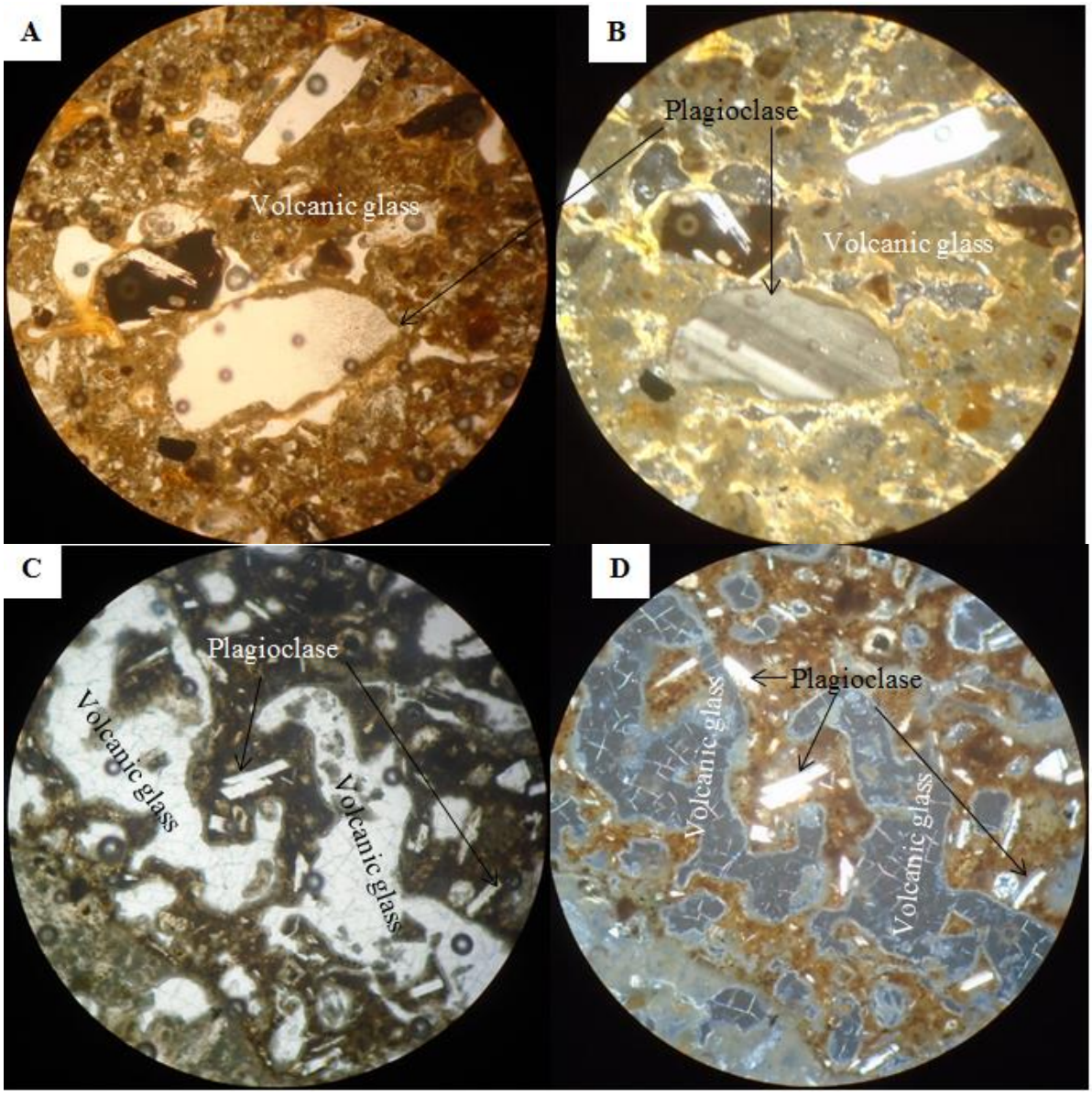

Figure 3.8: Microphotograph of the opal host rock of the area showing various mineralogical and textural features taken under 10*25 magnification power. Images, (A) and **(B)** are sample rhyolitic Ignimbrite (W-5), **(A)** were taken under plane polarized light and (B) were taken under crossed polarizers (XPL) showing large crystal of plagioclase; the plagioclase crystals are anhedral and the groundmass is dominated by brownish volcanic glass. Whereas **(C)** and **(D)** represent Sample W-6, rhyolitic Ignimbrite. **(C)** Were taken under plane polarized light and **(D)** Were taken under crossed polarizers (XPL) showing elongated crystal of plagioclase bounded with large proportion of volcanic glass filling the interstices of the mineral grains. The volcanic glass develops crack pattern which cross one another at around 90^0.

Sample no.	Rock texture	Rock name	Modal proportion	Mineral Texture
W-1	Pyroclastic (Vitrophyric Texture)	Rhyolitic Ignimbrite	Volcanic glass 70%	
			Quartz 5%	Anhedral
			Plagioclase 10%	Anhedral
			Chalcedony 10%	Radial-fibrous
			Pyroxene 2%	Anhedral
			Lithic-fragment 2%	Anhedral
			Opaque (Fe-oxide) 1%	Anhedral
W-2	Pyroclastic (Vitrophyric Texture)	Rhyolitic Ignimbrite	Volcanic glass 77%	
			Quartz 8%	Anhedral
			Chalcedony 5%	Radial-fibrous
			Biotite 4%	Anhedral
			Sanidine 3%	Anhedral
			Plagioclase 1%	Anhedral
			Opaque (Fe-Oxide) 2%	Anhedral
			Hornblende Trace	Anhedral
W-3	Pyroclastic (Vitrophyric Texture)	Rhyolitic Ignimbrite	Volcanic glass 78%	
			Quartz 9%	Anhedral
			Plagioclase 4%	Anhedral
			Chalcedony 3%	Radial-fibrous
			Opaque (Fe-Oxide) 2%	Anhedral
			Lithic-fragment 1%	Anhedral
			Sanidine 1%	Anhedral
			Hornblende Trace	Anhedral
		Rhyolitic	Volcanic glass 77%	

W-4	Pyroclastic (Vitrophyric Texture)	Ignimbrite	Quartz 12%	Anhedral
			Chalcedony 4%	Radial-fibrous
			Sanidine 3%	Anhedral
			Lithic-fragment 2%	Anhedral
			Hornblende 2%	Anhedral
			Opaque (Fe-Oxide) 1%	Anhedral
			Plagioclase 1%	Anhedral
W-5	Pyroclastic (Vitrophyric Texture)	Rhyolitic Ignimbrite	Volcanic glass 75%	
			Quartz 9 %	Anhedral
			Plagioclase 6%	Anhedral
			Opaque (Fe-Oxide) 4%	Anhedral
			Chalcedony 2%	Radial-fibrous
			Biotite 2%	Anhedral
			Sanidine 1%	Anhedral
			Hornblende Trace	Anhedral
W-6	Pyroclastic (Vitrophyric Texture)	Rhyolitic Ignimbrite	Volcanic glass 85%	
			Plagioclase 8%	Anhedral
			Opaque (Fe-Oxide) 3%	Anhedral
			Lithic-fragment 3%	Anhedral
			Pyroxene Trace	Anhedral

Table 3.1: Shows modal proportion and textures of the opal host rock of the study area.

CHAPTER FOUR RESULT AND DISCUSSION

4.1. INTRODUCTION

The samples are collected from three different local mining sites of Wegel Tena opal deposit (Koke Wuha to the northeast of Wegel Tena town, Anset to west of Wegel Tena town and Chegen to the north of Wegel Tena town). The collected samples have a code with a prefix of the locality name where they extracted, for example: - a prefix of "CH" stands for the sample extracted from Chegen locality. All samples are nodules of opal, sampled directly on the mining sites, then immediately stored in a closed plastic bottle with water and kept out of direct sunlight or intense light to prevent their possible destabilization.

4.2. BEHAVIOR OF SAMPLES BEFORE EXPOSURE TO AN OPEN AIR AND HEATING

KOK01 is a common colorless opal transparent and homogeneous, imprisoning balls of clay at its periphery and showing three Parallel network cracks. The local miners testify that this opal is highly unstable and after it is extracted and exposed to air with in few minutes it will develop a network of cracks.

KOK04 is a Colorless transparent opal, globally homogeneous, with a peripheral portion Pale yellow color with no visible cracks. According to the local miners, this opal is confusing with respect to its physical property; because after it is extracted for short period of time it start showing play of color but then through time it will start developing whitening and cracks.

KOK05 is a noble opal that is slightly translucent and homogeneous, covered with a thin clay layer having no cracks. The sample code KOK stand for all samples collected from Koke Wuha locality (see Gps location and local artisanal miner's testimony in table 4.1 bellow)

CH01 sample is extracted from Chegen locality which is around 17km to the north of Wegel Tena town. The sample is a transparent noble zoned opal, with an internal zone of fire opal and a bleached outer zone. The internal zone seems to develop light egg whitening.

AN02 sample is collected from Anset locality which is 12km to the west of Wegel Tena town. It is a common colorless opal slightly translucent and homogeneous, partially covered with clays on the surface with no crack initially. For this sample the local miner testify that, even if it doesn't show any play of color its stability is exceptional.

Sample no	Location	Locality name	Physical property of the samples (according to local miners)
KOK01	E-0525727 N-1281677 Elev-2772±8	Koke Wuha (northwest of Wegel Tena town)	Unstable colorless and transparent (will develop only crack within few mints after extraction)
KOK04	E-0525727 N-1281677 Elev-2772±8	Koke Wuha (northwest of Wegel Tena town)	Unstable colorless and transparent (will develop only crack within few mints after extraction)
KOK05	E-0525727 N-1281677 Elev-2772±8	Koke Wuha (northwest of Wegel Tena town)	Unstable translucent with high play of color (develop crack after extraction)
CH01	E-0531121 N-1294177 Elev-2949±6	Chegen (north of Wegel Tena town)	High play of color and Unstable (after extraction and expose to air automatically show random crack and whitening)
ANS02	E-0516600 N-1277339 Elev-2723±8	Anset (west of Wegel Tena)	Non transparent and highly stable (how much they stay in open air never develop crack or whitening)

Table 4.1: location and locality name of the place where the samples are extracted and their physical property according to the local artisanal miners' testimony.

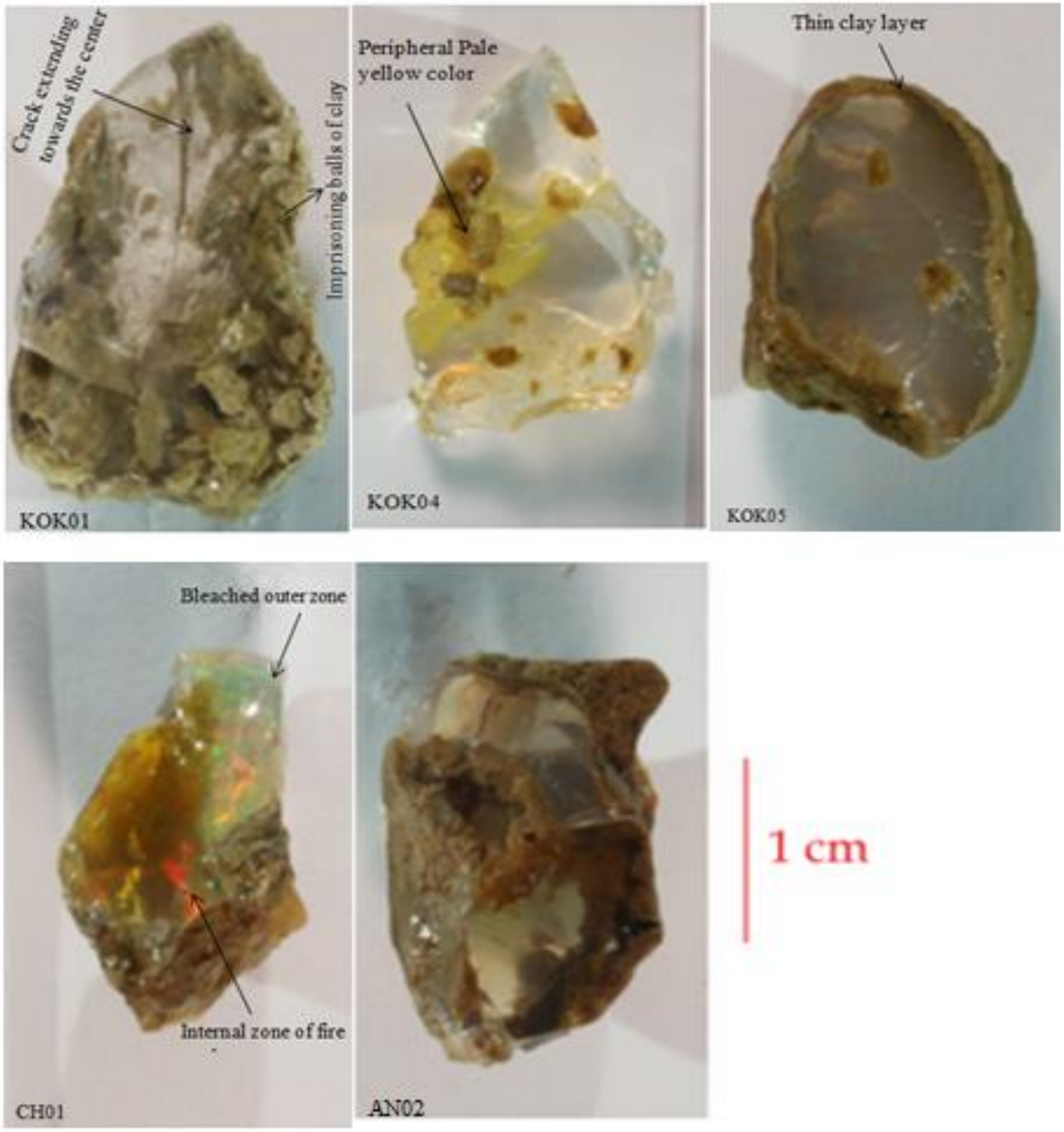

Figure 4.1: Samples of opals before exposure to open air and heating. From left to right: Koke Wuha 01; Koke Wuha 04; Koke Wuha 05; Chegen 01; Anset 02.

4.3. REACTION OF SAMPLES TO HEATING AND EXPOSURE TO THE OPEN AIR

In open air sample AN02 and KOK01 takes a few days and weeks respectively to reveal their hydrophane character. After they are heated at around 150^0C and exposed to laser the water evacuated very fast and their hydrophane character revealed within a second.

The non-hydrophane samples (KOK04, KOK05, internal zone of CH01) underwent intensive cracking after they heated. On the contrary hydrophane samples (KOK01, AN02, outer zone of CH01) do not crack or develop little crack. Generally heat causes more cracking than exposure to an open air within the body of the samples.

Sample	Characteristics	Initial state	Exposed to the air (Room temperature)	Heated at 150^0C
KOK01	Hydrophane Transparent	Three cracks Parallel network	Not cracked	Not cracked
KOK04	Non-hydrophane Transparent	Not cracked	Not cracked	Cracked Network centered
KOK05	Non-hydrophane Translucent	Cracked with polishing Parallelized network	Not cracked	Cracked Network centered
CH01 Fire Opal	Non-hydrophane Transparent (internal zone)	Not cracked	Cracked Cross cracks	Cracked Cross cracks
CH01 Bleached area	Hydrophane (periphery) Transparent	Not cracked	A crack Onion skin	Not cracked
AN02	Hydrophane Translucent	Not cracked	Not cracked	Not cracked (up to 500^0C)

Table 4.2: Behaviors of samples after heating and exposure to open air, depending on their characteristics several types of cracking have been observed (description in section 4.2). Cracking appears to be associated with the non-hydrophobic character.

After the samples are exposed to an air and heated, they developed three different types of cracking pattern (see figure 4.2 below). The prefabrication of KOK01as well as the cracking with polishing of KOK05 shows a network of curvilinear cracks that are globally parallel and transverse to the sense of elongation of the sample. The cracks are locally curved to join a neighbor crack which is close enough.

The cracking during the heating of the samples KOK04 and KOK05 is more abundant and branched. The crack network takes a centered shape that recalls the impact on safety glasses (Carre, 1996).

The cracking developed on CH01 is made of onion skin, following the interface between the zonations. It develops little in the bleached zone, but forms a network with crossed fissures in the internal zone of fire opal.

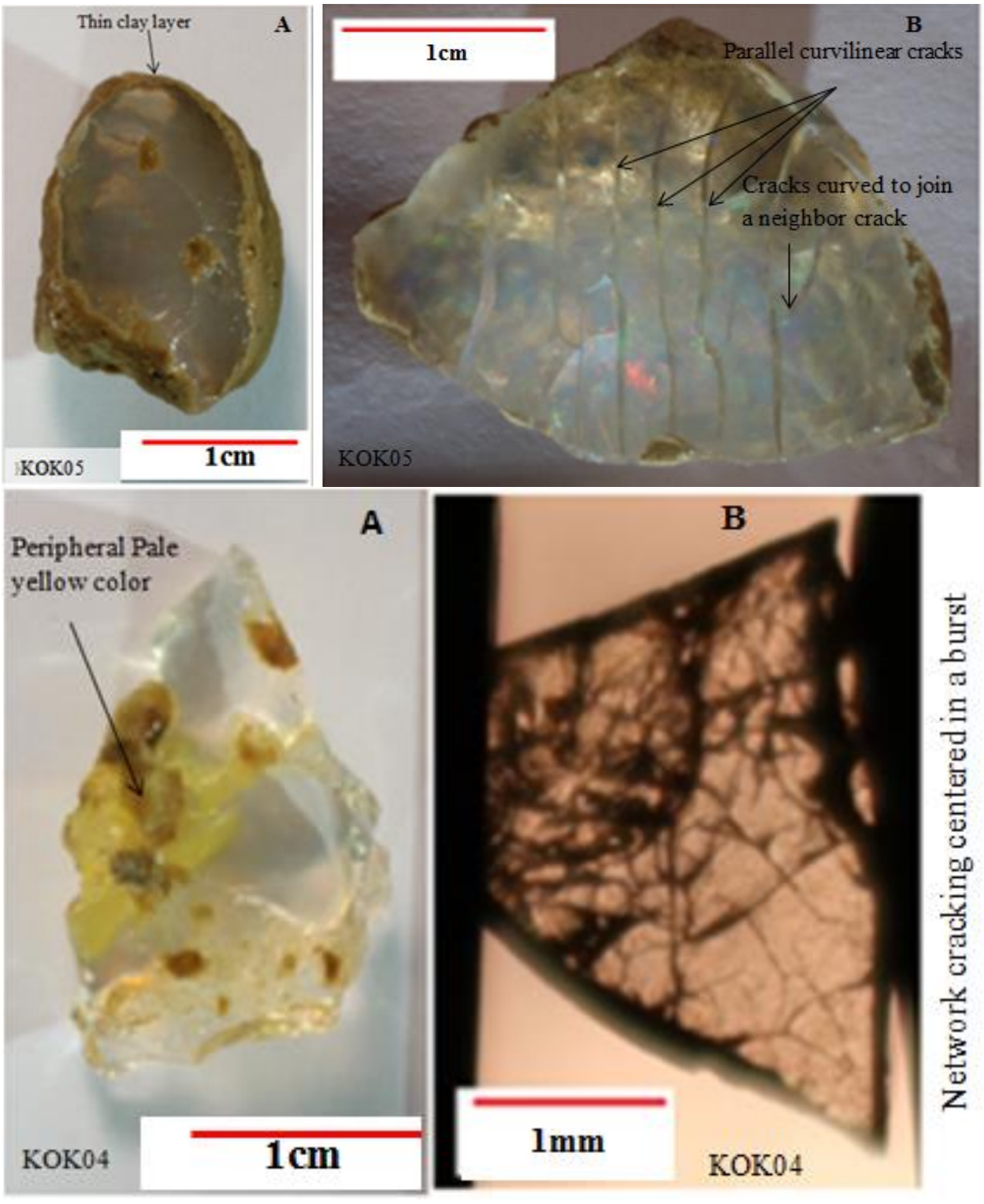
Thin clay layer
A
1cm
KOK05
1cm
B
Parallel curvilinear cracks
Cracks curved to join
a neighbor crack
KOK05
A
Peripheral Pale
yellow color
KOK04
1cm
B
1mm
KOK04
Network cracking centered in a burst

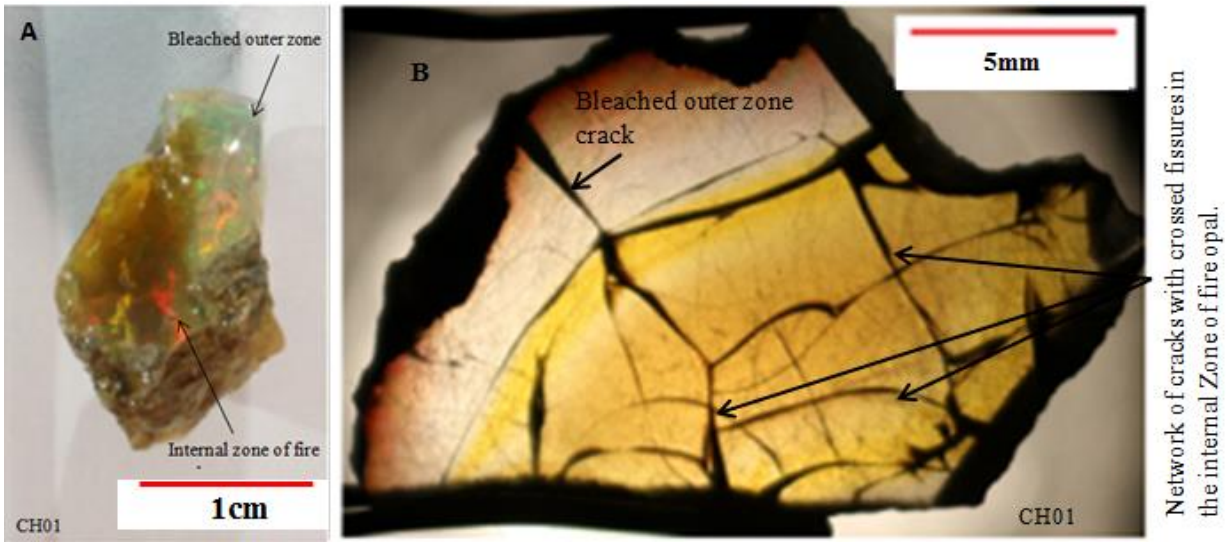

Figure 4.2: Photo KOK04 **(A),** KOK05 **(A)** and CH01 **(A)** Samples of opals before exposure to open air and heating. KOK04 **(B)** showing Network cracking centered in a burst, KOK05 **(B)** shows a network of curvilinear cracks that are globally parallel and transverse the cracks are locally curved to join a neighbor crack which is close enough; and CH01 **(B)** Differentiated cracking between zonation: marked in internal zone of fire opal, little cracks are marked in the bleached outer zone and is made of onion skin, following the interface between the zonation, but forms a network crack with crossed fissures in the internal zone of fire opal sample. Photographs KOK04 **(B)**, KOK05 **(B)** and CH01 **(B)** (Photographs have been taken in plane polarizer)

4.4. ABNORMAL BIREFRINGENCE PATTERNS

The occurrence of birefringence in cubic mineral is an anomalous optical property, which is the result of the photoelastic effect (Nye, 1957 and Poindexter, 1955) producing a change of refractive index with stress.

Opals are isotropic under normal condition but, observation of the opal samples in this work between crossed polarizers showed figures of abnormal birefringence after the cracks develops. This anisotropy is the control of stresses and deformations in the structure of the material (Howell, 2012).

In the current samples two types of abnormal birefringence pattern were observed (figure 4.3): Abnormal birefringence developed around defects (irregularities) on the surface of the samples and propagate over short distances (less than half-millimeter) towards the inside of the material. These irregularities can be the starting point for cracks (figure 4.3).

The second one, abnormal birefringence develops around the cracks, over a short distance (about a quarter of a millimeter). At the intersection of two cracks, anisotropic cross is formed, which follows the bisecting planes of the planes of the cracks. Abnormal birefringence develops around a crack and surface irregularities in KOK04 and around cracks in CH01.

The non-cracked samples of KOK04 do not exhibit abnormal birefringence (they are isotropes). Figures of abnormal birefringence appear with cracking. Cracking seems therefore to create anisotropy in the opal (Figure 4.4).

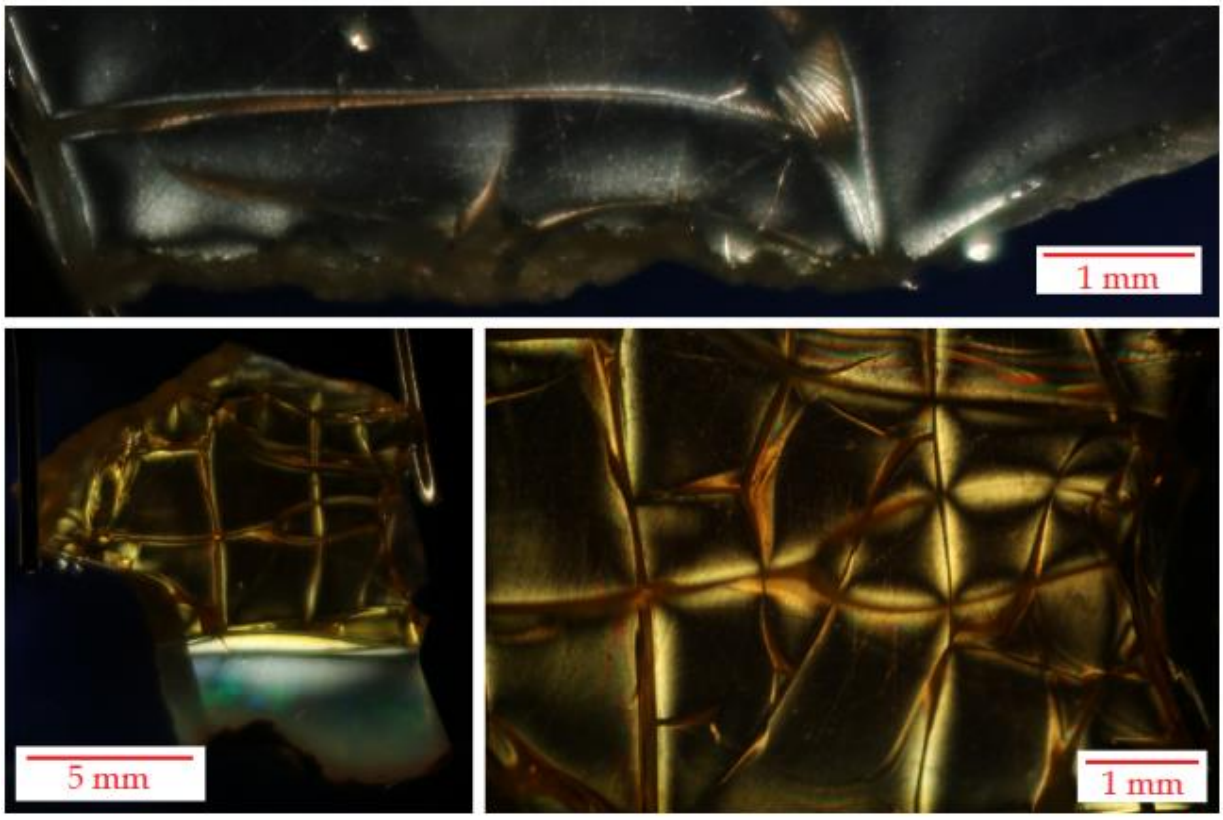

Figure 4.3: Top: abnormal birefringence around a crack and surface irregularities in KOK04. These irregularities correspond to points of cracks. Bottom left: abnormal birefringence

developed around cracks in CH01. These figures are wider in the bleached area, around the crack delimiting the two zones. Bottom right: zoom in the fire opal zone of CH01. Isotropic crosses are visible on the bisecting planes of the cracks. (Photographs have been taken under cross polarizers).

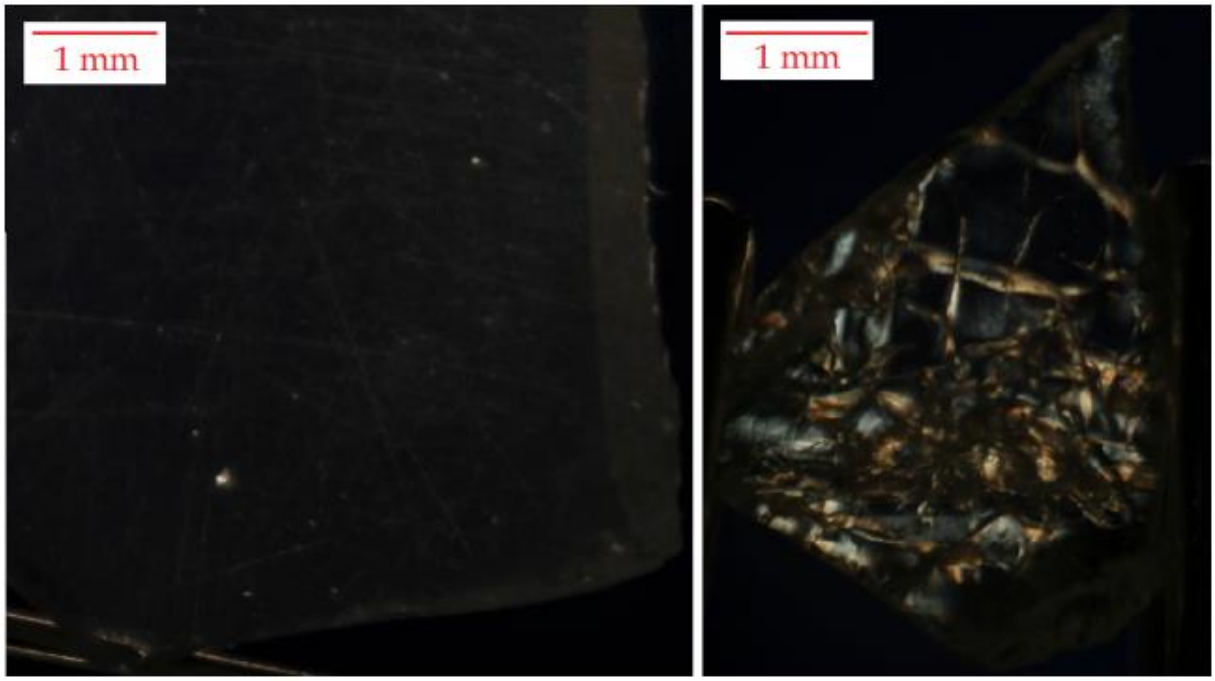

Figure 4.4: left KOK04 before heating and cracking: the sample shows an isotropy homogenous. To the right, KOK04 after heating and cracking: an abnormal birefringence appears around the cracks. (Photographs have been taken under cross polarizers).

4.5. RAMAN PROPERTIES OF THE OPAL SAMPLES

The Raman graph bellow showed us clear variations of the position of the Raman peaks of the studied opal at the surface of the samples at ambient temperature and after heating. Massive Raman spectrum centered between 325 and 328cm^{-1} for semi crystalline opal (Opal-CT) and between 410 cm^{-1} for amorphous opal (Opal-A) (Kiefert and Karampelas, 2011). All the samples analyzed here have massive Raman spectrum centered between 325 and 328 cm^{-1}.

Sample CH01 and KOK04 have position of Raman peaks between 775-785 and 772-785 respectively at ambient temperature. Ganesan et al. (1970) states that theoretical Opal-CT show a significant peak at 780cm^{-1}, which is resulted due to symmetrical elongation of Si-O-Si bond in the crystal structure. After the samples are heated at about 150^{o}C and cracked the

position of the average peaks in the Raman graphs are decreased to low wavenumbers in the analyzed samples. This negative shift relative to the unheated samples and the theoretical position of the peak at 780cm^{-1}, testifies to the creation of extensive constraints.

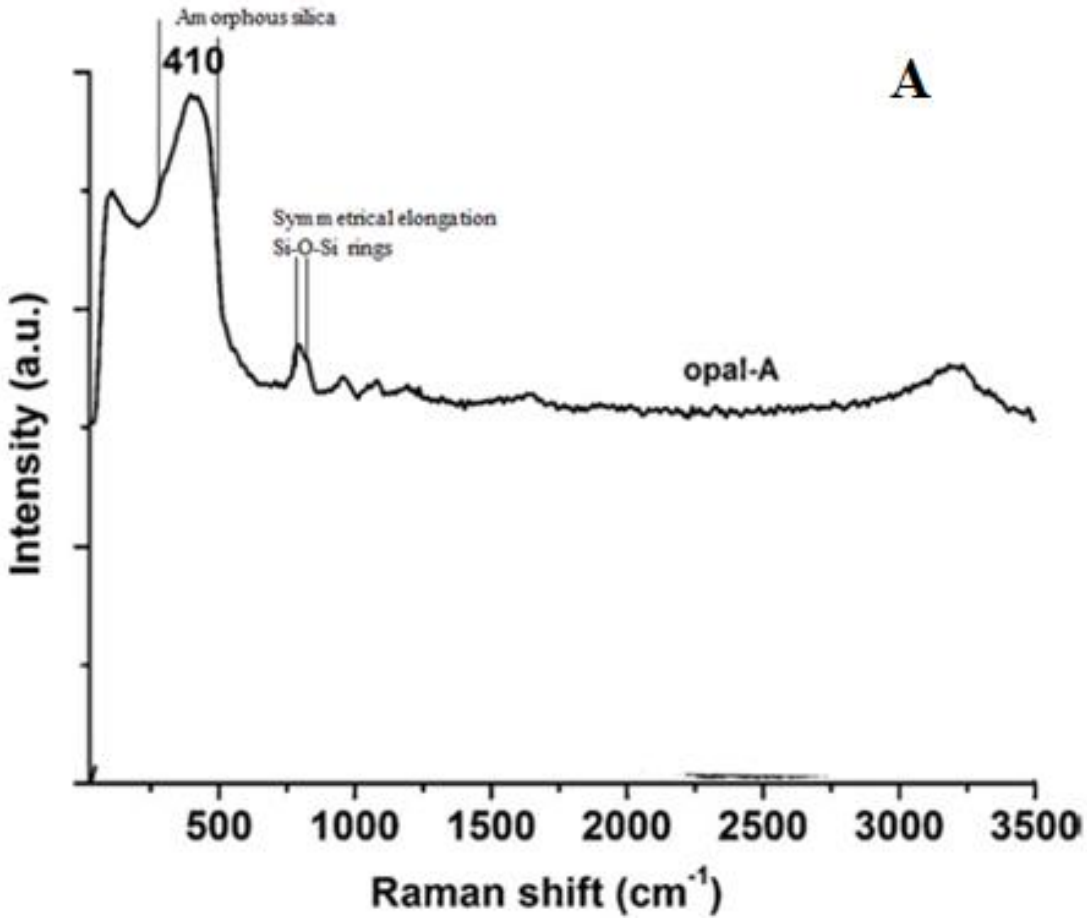

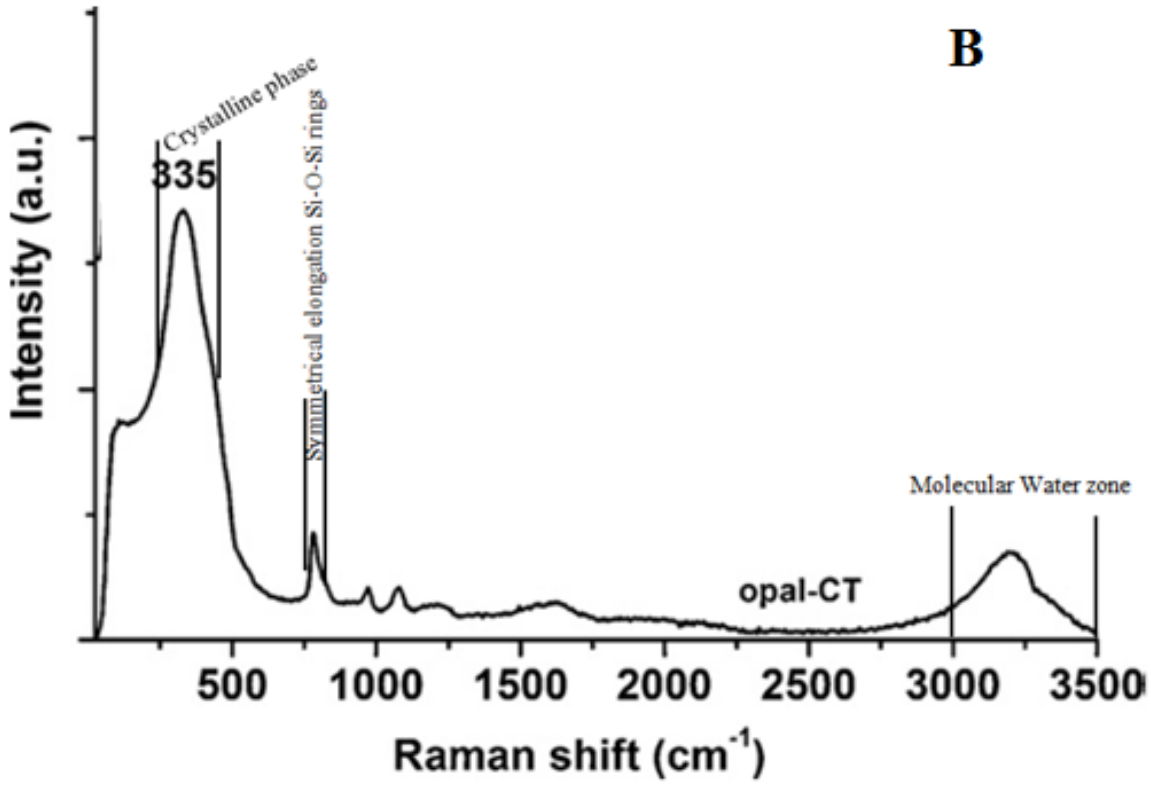

Figure 4.5: Raman spectra (excitation wavelength: 1064 nm, resolution: 4 cm^{-1}, 1000 scans) display a clear difference between opal-A (broad peak at about 410 cm^{-1}) and opal-CT (broad peak at about 355cm^{-1}). **(A)** In opal-A the Raman pick position at 410 cm^{-1} represent an amorphous nature of the opal. **(B)** Opal-CT broad peaks at 335 cm^{-1} represent crystalline phase opal. At 780cm^{-1} the Raman pick position shows symmetrical elongation of Si-O-Si bond in the crystal structure modified from Kiefert and Karampelas (2011).

Sample	T (˚C)	Cracking	Position min-max (cm^{-1})	Variation (cm^{-1})	Average Position (cm^{-1})	Shift (cm^{-1})
KOK01 Hydrophane	Ambiante 150	Cracked Not cracked	775-785 775-785	7 10	779.29 777.64	-1.65
KOK04	Ambiante 150	Not cracked Cracked	772-785 768-772	13 4	775.31 769.83	-5.48
KOK05	Ambiante 150	Not cracked Cracked	775-785	10	780.97 777.90	-3.07
CH01 Fire Opal	Ambiante 150	Not cracked Cracked	775-785 772-782	10 10	779.99 776.86	-3.10
AN02 Hydrophane	Ambiante 150	Not cracked Not Cracked	772-785	13	-	-

Table 4.3: Change in Raman properties depending on the heating and cracking state. Variations range from 4 to 13 cm^{-1}. They are observed whatever the hydrophobic character, the temperature or the state of cracking and shift of the mean peak position to780 cm^{-1} on the boards between the uncracked state and the cracked state. A downward shift wave's number is always observed when cracking occurs.

The average peak position of cracked CH01 sample decrease by 3.10cm^{-1} compared to the non-cracked samples. The cracked KOK04 sample shows the average peak position decrease by 5.48 cm^{-1} relative to the non-cracked sample.

The position of the peak at 780cm^{-1} is present in all samples, independently of the hydrophobic nature, the cracking state or the temperature. The heating does not directly affect

the distribution of stresses in the opal. Cracking appears to have a direct influence on the distribution of stresses in the opal. KOK01 does not present the mean shift of the peak at 780 cm -1 to the low numbers waves with temperature. Indeed, it is always associated with the displacement of the average of peak at 780cm^{-1} to the low wavenumbers.

The peak at 780cm^{-1} is the only one that shows significant variations in this study (Up to 13 cm^{-1} of variation). This peak is associated with the symmetric elongation of the Si-O-Si bond for the three or four member rings (Smallwood, 2000). In the silica glasses, the peak displacement at 800cm^{-1} is associated with the angular deformation of the Si-O-Si bond, considered to be the least resistant to deformation under stress (Tallant et al., 1988). Because of the proximity of the shape of the spectra of the silica glass and the opal I propose the following hypothesis: the Si-O-Si bond is the most deformed by the stresses in the opal, which is reflected by the significant variations of the peak at 780 cm^{-1} in the Raman shift graph.

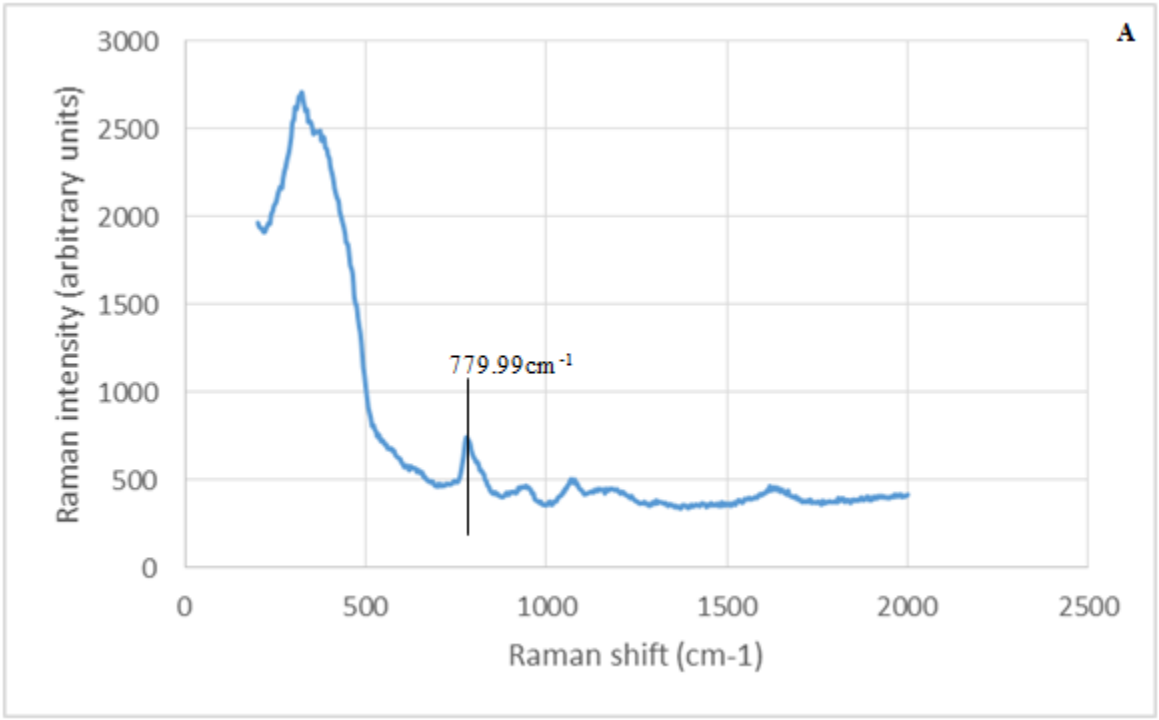

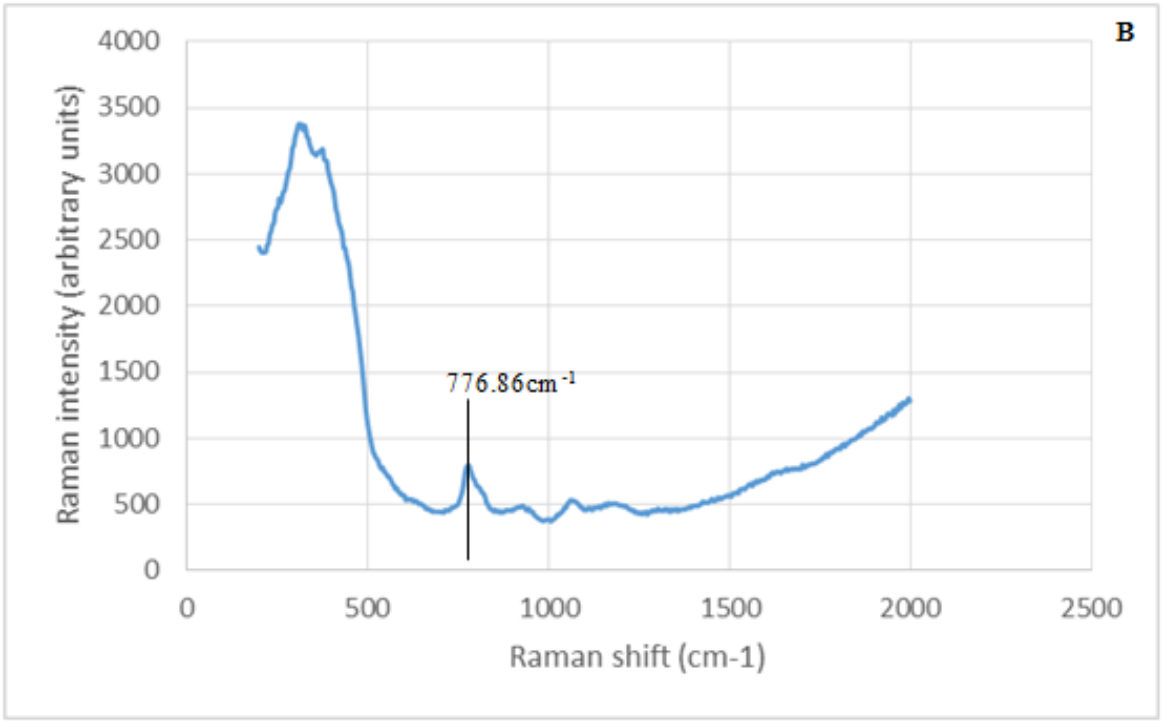

Figure 4.6: Raman spectra (excitation wavelength: 532nm, resolution: $3cm^{-1}$). **A)** Display Raman spectrum of CH01 before heating at ambient temperature and before cracking, peaks marked in black with Raman shift ($779.99cm^{-1}$) represent where the symmetrical elongation of Si-O-Si bond in the crystal structure of the opal. **B)** Raman spectrum of CH01after heating at 150^0C temperature and after the sample is cracked, peaks marked in black with Raman shift ($776.86cm^{-1}$) represent where the symmetrical elongation of Si-O-Si bond in the crystal structure of the opal. After the sample is heated at 150^0C and cracked it shows a negative Raman shift with ($-3.10cm^{-1}$) value from ($779.99cm^{-1}$to $776.86cm^{-1}$) which is related to significance Si-O-Si bond deformation by the stresses in the opal.

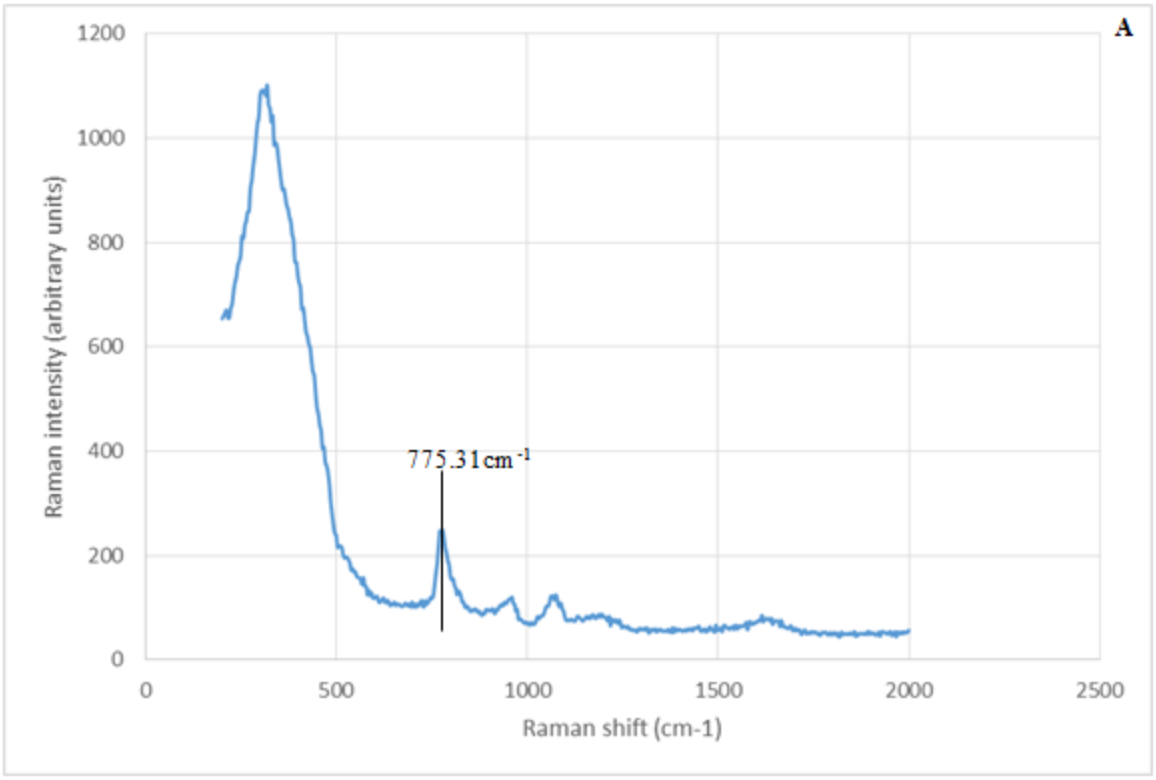
A
1200
1000
800
600
400
200
0
Raman intensity (arbitrary units)
775.31cm -1
0
500
1000
1500
2000
2500
Raman shift (cm-1)

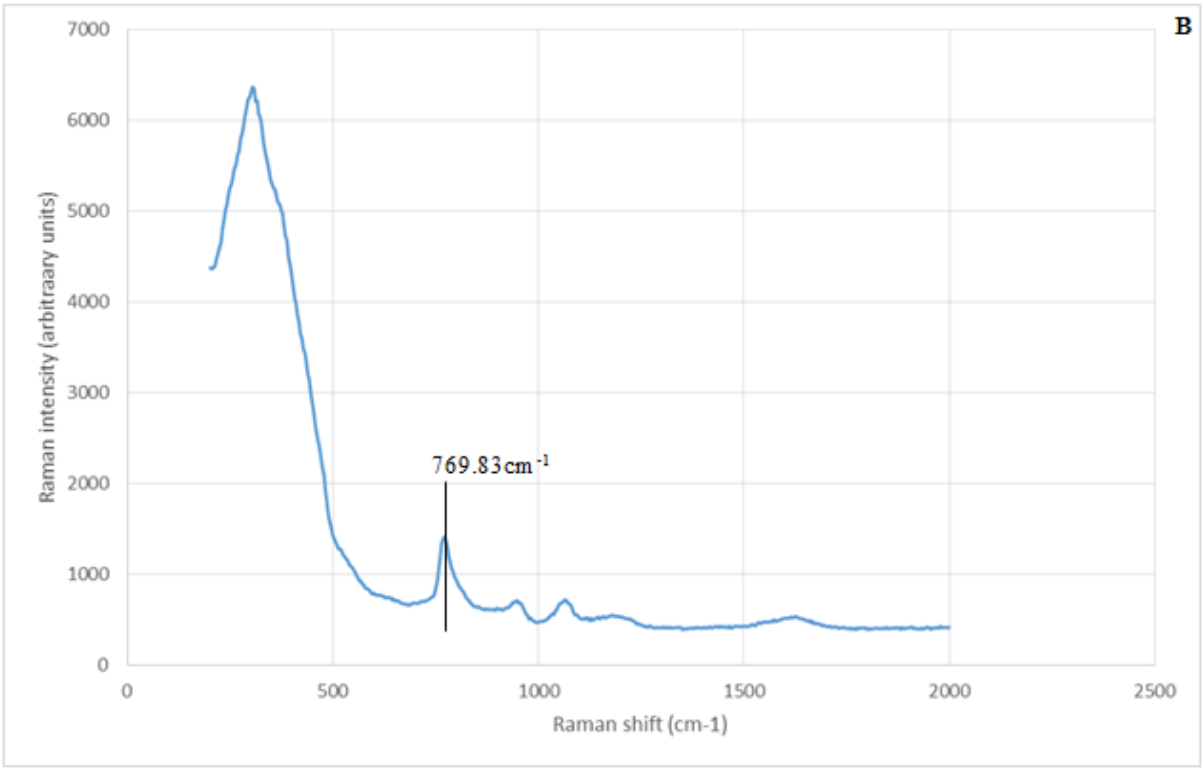
B
7000
6000
5000
4000
3000
2000
1000
0
Raman intensity (arbitraary units)
769.83cm -1
0
500
1000
1500
2000
2500
Raman shift (cm-1)

Figure 4.7: Raman spectra (excitation wavelength: 532nm, resolution: $3cm^{-1}$). **A)** Display Raman spectrum of KOK04 before heating at ambient temperature and before cracking, peaks marked in black with Raman shift ($775.31cm^{-1}$) represent where the symmetrical elongation of Si-O-Si bond in the crystal structure of the opal. **B)** Raman spectrum of KOK04 after heating at 150^0C temperature and after the sample is cracked, peaks marked in black with Raman shift ($769.83cm^{-1}$) represent where the symmetrical elongation of Si-O-Si bond in the crystal structure of the opal. After the sample is heated at 150^0C and cracked it shows a negative Raman shift with ($-5.48cm^{-1}$) value from ($775.31cm^{-1}$to $769.83cm^{-1}$) which is related to significance Si-O-Si bond deformation by the stresses in the opal.

4.6. GEMOLOGY AND CRAZING OF WOLLO OPALS

Almost all samples in crossed polarized light are initially isotropic and anisotropy is created around the cracks after the samples are heated. Around the cracks abnormal birefringence developed and they show interference pattern.

It is observed that evacuating water from non-hydrophane (KOK04, KOK05, internal zone of CH01) samples promotes cracking and cracked samples crack at heating, or show a propagation of cracks. I then propose the following hypotheses; the opal is isotropic between crossed polarizers, but is actually anisotropic on the microscopic scale. The evacuation of the water increases the stresses and creates surface shrinkage up to the cracking threshold, as Proposed by Filin and Puzynin (2009). Evacuating water from non-hydrophane samples promotes cracking. Also cracked samples can crack at heating, or show a propagation of new cracks. Hence in non-hydrophane samples water being linked to the silicate framework and the water detached from the internal structure, when the sample is heated and the water is being released it create enough internal stress and then lead to development of new cracks. Cracks then propagate from irregularities surface or from a pre-existing crack network. This assumption is consistent with the behavior of the glass, which presents stresses relocated around the point of the cracks that develop there (Carre, 1996). Diamond shows the same Property (Howell, 2012). Cracking relaxes the stresses by relocating them and homogenizing them around the cracks. This creates birefringence patterns (produce extensive local constraint) observed around the cracks between crossed polarizers. Continue to evacuate water from the opal can lead to a new cracking threshold and crack the opal. While the hydrophane opals (KOK01, CH01 bleach and AN02) do not crack because, the lost water is molecular not being linked to the silicate framework.

All hydrophane samples (KOK01, CH01 bleach and AN02) shows high resistance for cracking even at high temperature. Lab experiment by Chamard-Bois (2015) on the transformation of orange, transparent opal into white translucent and hydrophane opal by attacking soft chemical oxalic acid (bleaching chemical), he determined that oxalic acid complexes trivalent iron withdraws from opal and generates porosity in opal. The translucent nature of the opal is accompanied by the opening of a micro-porosity (Aguilar-Reyes, 2004)

and the existence of micro-porosity in hydrophane opal samples blocks the propagation of cracks within the body of the sample.

Rondeau et al. (2010) gives a general conclusion that, Wegel Tena translucent opal is more stable than transparent opal without considering there hydrophane character. However in this work one sample (KOK05) which is translucent underwent intensive cracking after heating. So the translucent nature of the sample is not the only property to be considered to analyses the crazing characteristic of opal. This implies hydrophane characteristics with translucent nature control the overall stability of opal.

Therefore Hydrophanes opals (KOK01, AN02, outer zone of CH01) have better resistance to cracking than non-hydrophanes opal, even at high temperatures. Very transparent opals however show the highest susceptibility to cracking (Rondeau et al., 2010). Chamard-Bois (2015) correlates the bleaching (translucent) with the hydrophane character and Aguilar-Reyes (2004) shows that the whitening (translucent) is accompanied by the opening of a micro-porosity. I therefore hypothesize that the micro-porosity developed in hydrophane samples transform the very transparent sample to translucent and blocks the development of cracking before the crack propagate.

CHAPTER FIVE CONCLUSION AND RECOMMENDATION

5.1. CONCLUSION

Cracking in the opal is a more complex phenomenon than one might at first think. While it seems to be linked with the loss of water probably molecular.

Non-hydrophane samples (KOK04, KOK05, internal zone of CH01) cracked at heating and exposed to air. Evacuating water from non-hydrophane samples promotes cracking. Also cracked samples can crack at heating or show a propagation of new cracks. Hence in non-hydrophane samples water being linked to the silicate framework and the water detached from the internal structure, when the sample is heated and the water is being released it create enough internal stress and then lead to development of new cracks. Cracking results either as a network global standard parallelized, either in the form of a centered network or as a network cross-crack.

Hydrophane samples (KOK01, AN02, outer zone of CH01) have better resistance to cracking than non-hydrophanes opals (KOK04, KOK05, internal zone of CH01) even at high temperature. In Hydrophane opals water exist in molecular form. Hence micro-porosity developed in hydrophane samples blocks the development of cracking.

Translucent nature of opal is not the only property to be considered to analyses the crazing (crack) characteristic of opal. This implies hydrophane characteristics with translucent nature control the overall stability of opal. The micro-porosity developed in hydrophane samples transform the very transparent sample to translucent and blocks the development of cracking before the crack propagates.

The Raman peak at 780cm^{-1} of the opal shows large variations (up to 13cm^{-1}) in the Raman spectra. These variations are present in all samples. It is always associated with the displacement of the average of peak at 780cm^{-1} to the low wavenumbers. This negative shift relative to the unheated samples and the theoretical position of the peak at 780 cm^{-1}, testifies to the creation of extensive constraints. The heating does not directly affect the distribution of stresses in the opal. Cracking appears to have a direct influence on the distribution of stresses in the opal. The stress distribution in the opal causes the deformation of the Si-O-Si bond. It is

distributed through opal, then relocates and homogenizes around cracks to appear in the form of extensive constraints.

Finally cracking relaxes the stresses by relocating them and homogenizing them around the cracks (produce extensive local constraint). This creates anisotropy around cracks and birefringence patterns observed around them between crossed polarizers. Abnormal birefringence figures appear with cracking, around surface irregularities or on the sides of the cracks.

5.2. RECOMMENDATION

There are some recommendations that rise relating with this study as follows:

- This research only concern understand cracking phenomenon of white transparent ,white translucent and fire opals I recommended for intended researchers better to study cracking phenomena of other type of opals.
- Very transparent non hydrophane opals are prone to cracks these defects make unsuitable for use in jewelry and influence the whole market of opal; therefore it would be better to study stabilizing mechanism (treatment) in order to cure it.
- The spectral resolution of this study is low resolution ($3cm^{-1}$), it only allows to record trends in the Raman peak position in $780cm^{-1}$ which do not reporting the overall behavior of the samples. It would also be interesting to see if other peaks correspond to high resolution, including the peaks of the water, beyond $2500\ cm^{-1}$. Therefore it would be useful to continue working on high resolution Raman spectroscopy.
- The mining techniques implied by the local miners are very traditional and it has a direct effect on the quality and stability of the mined opals so to avoid this, the mining techniques should be upgraded.

References

Aguilar-Reyes B.O. (2004). Microstructural study of opal: application to the destabilization by whitening. *PhD, University of Nantes*, 174.

Aguilar-Reyes B.O, Ostrooumov M., Fritsch E. (2005).Mineralogical study of the destabilization of Mexican opals. *Revis ta Mexicana de Ciencias Geol6gicas*. **22**(3): 391-400.

Ayalew, D., Yirgu, G., Barrey, P., Marty, B., Reisberg, L. and Pik, R. (2002). Source genesis and timing of giant ignimbrite deposits associated with Ethiopian continental flood basalts. *Geochemica et Cosmochimica Acta.* **66**: 1429-1448.

Ayalew, D. and Yirgu,G. (2003). Crustal contribution to the genesis of Ethiopian plateau rhyolitic ignimbrites: basalt and rhyolite geochemical provinciality. *Journal of the Geological Society, London* ,**160**: 47-56.

Baker, B. H., Mohr, P.A. and Williams, L.A.J. (1972). Geology of the east Africa. *Geological society of America special publication*,**136**: 67.

Berhe, S.M., Desta, B., Nicoletti, M. and Teferra, M. (1987). Geology, geochronology and geodynamics implications of the Cenozoic magmatic province in western and Southeastern Ethiopia. *J.Geol. Soc. London.* **144**: 213-226.

Behrens, H., Roux, J., Neuville, D. R. and Siemann, et M. (2006). Quantification of dissolves H_2O in silicate glasses using confocal microRaman spectroscopy. *Chemical Geology.* **229**(1–3): 96–112.

Carre, H. (1996). Study of Fracture Behavior of a Pre-stressed Fragile Material: Tempered Glass. *Doctoral thesis, National School of Roads and Bridges, Champs-sur-Marne (France).*175p.

Chamard-Bois, S. (2015). Bleaching of fire opals by oxalic acid .*Unpublished technical report, Laboratory of Planetology and Geodynamics of Nantes, France,* 1-65.

Davidson, A. (1983) The Omo river project, reconnaissance geology and geochemistry of parts of Ilubabor, Kefa, Gemu Gofa and Sidamo, Ethiopia. *Ethiop. Inst. Geol. Surv. Bull*. **2**: 1–89.

Elzea, J.M., and Rice, S.B.(1996). TEM and X-ray diffraction evidence for cristobalite and tridymite stacking sequences in opal. *Clays and Clay Minerals*. **44** (4): 492-500.

Filin, S.V. and Puzynin, A.l. (2009). Prevention of cracking in Ethiopian opal. *The Australian Gemmologist*. **23** (12):579-582.

Filin, S. V., Puzynin, A. I. and Samoilov, V. N. (2002). Some aspects of precious opal synthesis. *Australian Gemmologist* ,**21**: 278–282.

Fritsch, E., Rondeau, B., Ostrooumov, M., Lasnier, B., Marie, A. M., Barreau, A., Wery, Connoué, J., & Lefrant, S. (1999). Recent discoveries about opal. *Revue de Gemmologie afg*, **138/139**: 34-40.

Frondel, C. (1962). *The System of Mineralogy of James Dwight Dana and Edward Salisbury Dana, Yale University 1837-1892, Silica Minerals.* John Wiley & Sons, New York, **3**:334 pp.

Gaillou, E. (2006). Nanostructure Relations, Physical Properties and Formation Mode of Opals A and CT. *PhD thesis, University of Nantes, Nantes (France).*308 p.

Gaillou, E., Delaunay, A., Rondeau, B., Bouhnik-leCoz, M., Fritsch, E., Cornen, G., and Monnier,C. (2008). The geochemistry of gem opals as evidence of their origin. *Ore Geology Reviews*. **34** (1):113-126.

Ganesan, S., Maradudin, A. A. and Oitmaa, et J. (1970). A lattice theory of morphic effects in crystals of the diamond structure. *Annals of Physics.* **56**(2): 556–594.

Gauthier, J. P., Mazzero, F., Mandaba, Y., and Fritsch, E**.** (2004). Opal from Ethiopia: Usual gemology and unusual characteristics. *Revue de Gemmologie afg* .**149**: 15-23

George, R.M. and Rogers, N.W. (2002). Plume Dynamics beneath the African plate inferred from Geochemistry of the Tertiary Basalts of Southern Ethiopia. *Contrib mineral petrol.* **144**: 286-304.

Hatton, B., Mishchenko, L., Davis, S., Sandhage, K. H., and Aizenberg , et J. (2010). Assembly of large-area, highly ordered, crack-free inverse opal films. *Proceedings of the National Assembly of Sciences of the United States of America* .**107**(23): 10354–10359.

Hofmann, C., Courtillot, V., Féraud, G., Rochette, P., Yirgu, G., Ketefo, E. and Pik, R.,(1997).Timing of the Ethiopian flood basalt event and implications for plume birth and global change. *Nature* **389** :838–841.

Howell, D. (2012). Strain-induced birefringence in natural diamond: a review. *European Journal of Mineralogy* .**24**(4): 575–585.

Howell, D., Wood, I. G. Dobson, D. P. Jones, A. P. Nasdala, L. and Harris, J.W. (2010). Quantifying strain birefringence halos around inclusions in diamond. *Contributions to Mineralogy and Petrology* .**160**(5):705–717.

Ivanov, V. G., Faulques, E., Aguilar, B. & Fritsch, E. (2004). Raman Markers for $(SiO)_6$ Rings in Opals: *Evidences and Implications*.

Jones, JB., and Segnit, ER. (1971) .The nature of opal I. Nomenclature and constituent phases. *J Geol Soc Aust*. **18** :57-68.

Kazmin, V. (1972). The Geology of Ethiopia Unpublished report, *EIGS*, Addis Ababa, Ethiopia.

Kiefert, L. and Karampelas, S. (2011). "Use of the Raman spectrometer in gemological laboratories: review," *Spectrochim. Acta Part A* 80, 119–124

Kurkura, K.(2010). Geological and geochemical variations in Mid-Tertiary Ethiopian Flood Basalt Province, Maychew, Tigray Region, Ethiopia. *CNCS. **2** (1):* 4-25.

Lang, AR. (1967). Causes of birefringence in diamond. *Nature* .**213**:248–251.

LeLosq, C., and Neuville, D. R. (2013). Effect of the Na/K mixing on the structure and the rheology of tectosilicate silica-rich melts. *Chemical Geology*, **346**:**57**-71.

LeLosq, C., Neuville, D. R., Florian, P., Henderson, G. S., and Massiot, D. (2014). The role of Al^{3+} on rheology and structural changes in sodium silicate and aluminosilicate glasses and melts. *Geochimica et Cosmochimica Acta* .**126**: 495-517.

Luigi, B., Gianluca, B., Claudio, N. and Franca, S. (2009). Continental Flood Basalts and Mantle Plumes: a Case Study of the Northern Ethiopian Plateau. *Journal of Petrology.*

Marc ,D., Ian P. and Nick R.(2003?). The Origin of High-Ti Picrites from the Ethiopian Flood Basalt Province. *The Department of Earth Sciences, The Open University, Walton Hall, Milton Keynes MK7 6AA.*

Mary, L. J., Robert, C. K., Dino, G. D., and John, I. K. (1996). Opal from Shewa province, Ethiopia. *Gems & Gemology*. **32**(2): 112-120.

Mazzero , F., Gauthier, J.-P., Rondeau, B., Fritsch ,E., and Bekele E. (2009). New deposit of Ethiopian opals in Wello Province: Early information. *Revue de Gemmologie a.f.g*., No.167:4-5.

Mazzero, F., Désagulier, C., Rondeau, B., Ayalew, D., Ezezew, G., Cenki, T., and Bekele, E. (2010). The opal of Wollo, Ethiopia: mines deposits. *Review of Gemmology afg.***174**: 14-20.

Mengesha, T., Tadiwos, C. and Workineh, H. (1996). *Exploration of the Geological map of Ethiopia,* 2nd ed., institute of mine and energy, Ethiopia, 83pp.

Merla, G. & Abbate, E. et al.(1979). A Geological Map of Ethiopia and Somalia (1973) and *Comment with a Map of Major Landforms. CNR*, Florence.

Mohr,P.A. (1962). The Geology of Ethiopia. *University. Coll of Addis Ababa press*. (reprinted in 1971 Haileselassie University press), Asmera , Ethiopia. 268pp

Mohr,P.A.(1963). The Geological map of the Horn of Africa, 2,000,000 scale. *Philip and Jaccy, London.*

Mohr, P. and Zanettin, B. (1988). The Ethiopian flood basalt province. In: Macdougall, J.D. (ed.), Continental flood basalts, *Kluwer Academic Publishers, Dordrecht*. 63-110.

Nye, JF. (1957). Physical properties of crystals. *Oxford Science Publications*, Oxford.

Ostrooumov, M., Fritsch, E., Lasnier, B., & Lefrant, S. (1999). Raman spectra of opals; aspect diagnostic and classification assistance. *European Journal of Mineralogy*. **11**(5): 899-908.

Ostrooumov, M.(2007). A Raman, infrared and XRD analysis of the instability in volcanic opals from Mexico. *Spectrochimica Acta Part A.* **68**:1070–1076.

Paris, M., Fritsch E. and Aguilar Rayes B.O. (2006). ^{1}H, ^{29}Si and ^{27}Al NMR study of the destabilization process of a paracrystalline opal from Mexico. *Journal of Non-Crystalline Solids* .**353***:*1650–1656.

Pearson G. (1985). Role of water in cracking of opal. *The Australian Gemologist* .**15**(12): 435-445.

Pik, R., Deniel, C., Coulon, C., Yirgu, G., Hofmann, C. & Ayalew, D.(1998).The northwestern Ethiopian plateau flood basalts: classification and spatial distribution of magma types. *Journal of Volcanology and Geothermal Research*, **81**: 91–111.

Poindexter E. (1955). Piezobirefringence in diamond. *Am Mineral* .**40**:1032–1054.

Rey, P. F. (2013). Opalisation of the Great Artesian Basin (central Australia): an Australian story with a Martian twist. *Australian Journal of Earth Sciences*, **60** (3): 291-314.

Rochette, E., Tamrat, E., Fraud, G., Pik, R., Courtillot, V. and Ketefo, E. (1998). Magneto stratigraphy and timing of the Oligocene Ethiopian traps. *Earth and Planetary Science letter.* **164**: 497-510.

Rondeau, B., Cenki-Tok, B., Fritsch, E., Mazzero, F., Gauthier, J. P., Bodeur, Y., Bekele, E., Gaillou, E. & Ayalew, D. (2012). Geochemical and petrological characterization of gem opals from Wegel Tena, Wollo, Ethiopia: opal formation in an Oligocene soil. *Geochemistry: Exploration, Environment, Analysis.* **12(**2):93-104.

Rondeau, B., Fritsch, E., Mazzero, F., and Gauthier, et J. P.(2011a). Opal- The Craze for Stability. *InColor, International colored Gemstone Association,* 42-45.

Rondeau, B., Fritsch, E., Bodeur,Y.,Mazzero ,F., Cenki ,T., Bekele ,E., Ayalew ,D., Cenki-Tok ,B., and Gsuyhier ,J.P. (2011b) .Wollo opals- A powerful source from Ethiopia. *InColor*: 24-34.

Rondeau B., Mazzero F., Bekele E., Gauthier J.-P., Fritsch E. (2010). Play-of-color opal from Wegeltena, Wollo province, Ethiopia. *Gems& Gemology* **46** (2): 90-105.

Rondeau, B.,Gauthier,J.P., Francesco Mazzero. F., Fritsch,E., Bodeur,Y., and Chauviré,B. (2013). On the origin of digit patterns in gem opal, G*ems & gemology*. **49**(3):138–146.

Rossano, S., and Mysen, B. O. (2013). Raman spectroscopy of silicate glasses and melts in geological systems. *Raman Spectroscopy Applied to Earth Sciences and Cultural Heritage (EMU Notes in Mineralogy*. **12**: 321-366.

Rosenfeld, JL. and Chase, AB. (1961) Pressure and temperature of crystallization from elastic effects around solid inclusions in minerals? *Am J Sci* . **259**:519–541.

Rus, L., Rada, S., Rednic, V., Culea, E., Rada, M., Bot, A., Aldea, N. and Rusu, T. (2014). Structural and optical properties of the lead based glasses containing iron (III) oxide. *Journal of Non-Crystalline Solids*. **402**:111-115.

Sanders, J.V. (1964). Colour of precious opal. *Nature*, **204**: 1151 – 1153.

Seid Ali. (2006).Origin of opal Hosted in Volcanic Rocks At Koste – Amba and Gift Mariyam,North Shoa (Central – Eastern Ethiopia). Unpublished MSc Thesis, Addis Ababa University, Addis Ababa, Ethiopia, pp 102.

Segnit, E. R., Stevens, T. J., and Jones, J. B. (1965). The role of water in opal. *Journal of the Geological Society of Australia: An International Geoscience Journal of the Geological Society of Australia*. **12**(2): 211-226.

Smallwood, A. (2000). A preliminary investigation of precious opal by laser Raman spectroscopy. *Australian Gemmologist* 20, 363–366.

Smith KL.(1988). Opals from Opal Butte, Oregon. *Gems & Gemology*. **24(**4):229-236.

Solomon Gerra. (2000). A short introduction to the geology of Ethiopia, *Chronique de la Recherche minieral Na.* **540**: 2000, 3-10.

Strubbe, D.A., Johlin, E.C., Kirkpatrick, T.R., Buonassisi, T. and Grossman, et J.C. (2015). Stresseffects on the Raman spectrum of an amorphous material: theory and experiment on a-Si :H. *Physical Review B.* **92**(24) :1-20.

Tallant, D. R., Michalske, T. A. and Smith. et W. L. (1988). The effects of tensile stress on the Raman spectrum of silica glass. *Journal of Non-Crystalline Solids.* **106**(1–3), 380–383.

Tesfaye, D., Genet, Y., Abraham, M., Yibeltal, T., Yonas, T., Getachew B., Mohammed, E. and Meran W. (2010).Geology Geochemistry and gravity survey of the Dessie area. *Ethiopian Institute of Geological Surveys, unpublished report Addis Ababa,*76.

Tefera, M., Chernet, T. & Haro, W. (1996). Explanation of the Geological Map of Ethiopia .*Ethiopian Institute of Geological Surveys, Addis Ababa*, **3**:79.

Wilson, M. J. (2014). The structure of opal-CT revisited. *Journal of Non-Crystalline Solids*. **405** : 68-75.

Zanettin , B, Justin Visentin E, Nicoletti M, Piccirillo EM, Carrelli, A. (1980) Correlations among Ethiopian volcanic formations with special references to the chronological and stratigraphical problems of the ‘‘Trap Series’’. Geodynamic evolution of the Afro-Arabian Rift System. *Atti dei convegni lincei*. **47**: 231–252.

DECLARATION

This Thesis is my original work and has not been presented for a degree in any other University and that all sources of material used for the thesis have been accordingly acknowledged.

Selamawit Dagnachew

Signature _____ date _____

This thesis has been submitted for examination with my approval as university advisors.

Professor Dereje Ayalew

Signature _____ date _____

Dr. Worash Getaneh

Signature _____ date _____

Date and place of submission: November / 2017, Addis Ababa, Ethiopia

Originality of this research work cheeked on free plagiarism checker website (https://www.paperrater.com/plagiarism-checker) and the results are presented bellow in separate chapter as follows.

Chapters	originality
Chapters 1	100%
Chapters 2	95%
Chapters 3	100%
Chapters 4	100%
Chapters 5	100%